Reusing label functions to extract multiple types of relationships from biomedical abstracts at scale

Authors

- **David N. Nicholson**
  [0000-0003-0002-5761](#) · [danich1](#)
  Department of Systems Pharmacology and Translational Therapeutics, University of Pennsylvania · Funded by GBMF4552

- **Daniel S. Himmelstein**
  [0000-0002-3012-7446](#) · [dhimmel](#) · [dhimmel](#)
  Department of Systems Pharmacology and Translational Therapeutics, University of Pennsylvania · Funded by GBMF4552

- **Casey S. Greene**
  [0000-0001-8713-9213](#) · [cgreene](#) · [GreeneScientist](#)
  Department of Systems Pharmacology and Translational Therapeutics, University of Pennsylvania · Funded by GBMF4552 and R01 HG010067

Abstract

Knowledge bases support multiple research efforts such as providing contextual information for biomedical entities, constructing networks, and supporting the interpretation of high-throughput analyses. Some knowledge bases are automatically constructed, but most are populated via some form of manual curation. Manual curation is time consuming and difficult to scale in the context of an increasing publication rate. A recently described "data programming" paradigm seeks to circumvent this arduous process by combining distant supervision with simple rules and heuristics written as labeling functions that can be automatically applied to inputs. Unfortunately writing useful label functions requires substantial error analysis and is a nontrivial task: in early efforts to use data programming we found that producing each label function could take a few days. Producing a biomedical knowledge base with multiple node and edge types could take hundreds or possibly thousands of label functions. In this paper we sought to evaluate the extent to which label functions could be re-used across edge types. We used a subset of Hetionet v1 that centered on disease, compound, and gene nodes to evaluate this approach. We compared a baseline distant supervision model with the same distant supervision resources added to edge-type-specific label functions, edge-type-mismatch label functions, and all label functions. We confirmed that adding additional edge-type-specific label functions improves performance. We also found that adding one or a few edge-type-mismatch label functions nearly always improved performance. Adding a large number of edge-type-mismatch label functions produce variable performance that depends on the edge type being predicted and the label function's edge type source. Lastly, we show that this approach, even on this subgraph of Hetionet, could add new edges to Hetionet v1 with high confidence. We expect that practical use of this strategy would include additional filtering and scoring methods which would further enhance precision.

Introduction

Knowledge bases are important resources that hold complex structured and unstructed information. These resources have been used in important tasks such as network analysis for drug repurposing discovery [1,2,3] or as a source of training labels for text mining systems [4,5,6]. Populating knowledge bases often requires highly-trained scientists to read biomedical literature and summarize the results [7]. This manual curation process requires a significant amount of effort and time: in 2007 researchers estimated that filling in the missing annotations would require approximately 8.4 years [8]. The rate of publications has continued to increase exponentially [9]. This has been recognized as a considerable challenge, which can lead to gaps in knowledge bases [8].

Relationship extraction has been studied as a solution towards handling this problem [7]. This process consists of creating a machine learning system to automatically scan and extract relationships from textual sources. Machine learning methods often leverage a large corpus of well-labeled training data, which still requires manual curation. Distant supervision is one technique to sidestep the requirement of well-annotated sentences: with distant supervision one makes the assumption that all sentences containing an entity pair found in a selected database provide evidence for a relationship [4]. Distant supervision provides many labeled examples; however it is accompanied by a decrease in the quality of the labels.

Ratner et al. [10] recently introduced "data programming" as a solution. Data programming combines distant supervision with the automated labeling of text using hand-written label functions. The distant supervision sources and label functions are integrated using a noise aware generative model that is used to produce training labels. Combining distant supervision with label functions can dramatically reduce the time required to acquire sufficient training data. However, constructing a knowledge base of heterogeneous relationships through this framework still requires tens of hand-written label functions for each relationship type. Writing useful label functions requires significant error analysis, which can be a time-consuming process.

In this paper, we aim to address the question: to what extent can label functions be re-used across different relationship types? We hypothesized that sentences describing one relationship type may share information in the form of keywords or sentence structure with sentences that indicate other relationship types. We designed a series of experiments to determine the extent to which label function re-use enhanced performance over distant supervision alone. We examined relationships that indicated similar types of physical interactions (i.e., gene-binds-gene and compound-binds-gene) as well as different types (i.e., disease-associates-gene and compound-treats-disease). The re-use of label functions could dramatically reduce the number required to generate and update a heterogeneous knowledge graph.

Related Work

Relationship extraction is the process of detecting and classifying semantic relationships from a collection of text. This process can be broken down into three different categories: (1) the use of natural language processing techniques such as manually crafted rules and the identification of key text patterns for relationship extraction, (2) the use of unsupervised methods via co-occurrence scores or clustering, and (3) supervised or semi-supervised machine learning using annotated datasets for the classification of documents or sentences. In this section, we discuss selected efforts for each type of edge that we include in this project.

Disease-Gene Associations

Efforts to extract Disease-associates-Gene (DaG) relationships have often used manually crafted rules or unsupervised methods. One study used hand crafted rules based on a sentence's grammatical structure, represented as dependency trees, to extract DaG relationships [11]. Some of these rules inspired certain DaG text pattern label functions in our work. Another study used co-occurrence frequencies within abstracts and sentences to score the likelihood of association between disease and gene pairs [12]. The results of this study were incorporated into Hetionet v1 [3], so this served as one of our distant supervision label functions. Another approach built off of the above work by incorporating a supervised classifier, trained via distant supervision, into a scoring scheme [13]. Each sentence containing a disease and gene mention is scored using a logistic regression model and combined using the same co-occurrence approach used in Pletscher-Frankild et al. [12]. We compared our results to this approach to measure how well our overall method performs relative to other methods. Besides the mentioned three studies, researchers have used co-occurrences for extraction alone [14,15,16] or in combination with other features to recover DaG relationships [17]. One recent effort relied on a bi-clustering approach to detect DaG-relevant sentences from Pubmed abstracts [18] with clustering of dependency paths grouping similar sentences together. The results of this work supply our domain heuristic label functions. These approaches do not rely on a well-annotated training performance and tend to provide excellent recall, though the precision is often worse than with supervised methods [19,20].

Hand-crafted high-quality datasets [21,22,23,24] often serve as a gold standard for training, tuning, and testing supervised machine learning methods in this setting. Support vector machines have been repeatedly used to detect DaG relationships [21,25,26]. These models perform well in large feature spaces, but are slow to train as the number of data points becomes large. Recently, some studies have used deep neural network models. One used a pre-trained recurrent neural network [27], and another used distant supervision [28]. Due to the success of these two models, we decided to use a deep neural network as our discriminative model.

Compound Treats Disease

The goal of extracting Compound-treats-Disease (CtD) edges is to identify sentences that mention current drug treatments or propose new uses for existing drugs. One study combined an inference

model from previously established drug-gene and gene-disease relationships to infer novel drug-disease interactions via co-occurrences [29]. A similar approach has also been applied to CtD extraction [30]. Manually-curated rules have also been applied to PubMed abstracts to address this task [31]. The rules were based on identifying key phrases and wordings related to using drugs to treat a disease, and we used these patterns as inspirations for some of our CtD label functions. Lastly, one study used a bi-clustering approach to identify sentences relevant to CtD edges [18]. As with DaG edges, we use the results from this study to provide what we term as domain heuristic label functions.

Recent work with supervised machine learning methods has often focused on compounds that induce a disease: an important question for toxicology and the subject of the BioCreative V dataset [32]. We don't consider environmental toxicants in our work, as our source databases for distant supervision are primarily centered around FDA-approved therapies.

Compound Binds Gene

The BioCreative VI track 5 task focused on classifying compound-protein interactions and has led to a great deal of work on the topic [33]. The equivalent edge in our networks is Compound-binds-Gene (CbG). Curators manually annotated 2,432 PubMed abstracts for five different compound protein interactions (agonist, antagonist, inhibitor, activator and substrate/product production) as part of the BioCreative task. The best performers on this task achieved an F1 score of 64.10% [33]. Numerous additional groups have now used the publicly available dataset, that resulted from this competition, to train supervised machine learning methods [27,34,35,36,36,37,38,39,40] and semi-supervised machine learning methods [41]. These approaches depend on well-annotated training datasets, which creates a bottleneck. In addition to supervised and semi-supervised machine learning methods, hand crafted rules [42] and bi-clustering of dependency trees [18] have been used. We use the results from the bi-clustering study to provide a subset of the CbG label functions in this work.

Gene-Gene Interactions

Akin to the DaG edge type, many efforts to extract Gene-interacts-Gene (GiG) relationships used co-occurrence approaches. This edge type is more frequently referred to as a protein-protein interaction. Even approaches as simple as calculating Z-scores from PubMed abstract co-occurrences can be informative [43], and there are numerous studies using co-occurrences [16,44,45,46]. However, more sophisticated strategies such as distant supervision appear to improve performance [13]. Similarly to the other edge types, the bi-clustering approach over dependency trees has also been applied to this edge type [18]. This manuscript provides a set of label functions for our work.

Most supervised classifiers used publicly available datasets for evaluation [47,48,49,50,51]. These datasets are used equally among studies, but can generate noticeable differences in terms of performance [52]. Support vector machines were a common approach to extract GiG edges [53,54]. However, with the growing popularity of deep learning numerous deep neural network architectures have been applied [41,55,56,57]. Distant supervision has also been used in this domain [58], and in fact this effort was one of the motivating rationales for our work.

Materials and Methods

Hetionet

Figure 1: A metagraph (schema) of Hetionet where biomedical entities are represented as nodes and the relationships between them are represented as edges. We examined performance on the highlighted subgraph; however, the long-term vision is to capture edges for the entire graph.

Hetionet [3] is a large heterogenous network that contains pharmacological and biological information. This network depicts information in the form of nodes and edges of different types: nodes that represent biological and pharmacological entities and edges which represent relationships between entities. Hetionet v1.0 contains 47,031 nodes with 11 different data types and 2,250,197 edges that represent 24 different relationship types (Figure 1). Edges in Hetionet were obtained from open databases, such as the GWAS Catalog [59] and DrugBank [60]. For this project, we analyzed performance over a subset of the Hetionet relationship types: disease associates with a gene (DaG), compound binds to a gene (CbG), gene interacts with gene (GiG) and compound treating a disease (CtD).

Dataset

We used PubTator [61] as input to our analysis. PubTator provides MEDLINE abstracts that have been annotated with well-established entity recognition tools including DNorm [62] for disease mentions, GeneTUKit [63] for gene mentions, Gnorm [64] for gene normalizations and a dictionary based search system for compound mentions [65]. We downloaded PubTator on June 30, 2017, at which point it contained 10,775,748 abstracts. Then we filtered out mention tags that were not contained in hetionet. We used the Stanford CoreNLP parser [66] to tag parts of speech and generate dependency trees. We extracted sentences with two or more mentions, termed candidate sentences. Each candidate sentence was stratified by co-mention pair to produce a training set, tuning set and a testing set (shown in Table 1). Each unique co-mention pair is sorted into four categories: (1) in hetionet and has sentences, (2) in hetionet and doesn't have sentences, (3) not in hetionet and does have sentences and (4) not in hetionet and doesn't have sentences. Within these four categories each pair is randomly assigned their own individual partition rank (continuous number between 0 and 1).

Any rank lower than 0.7 is sorted into the training set, while any rank greater than 0.7 and lower than 0.9 is assigned to the tuning set. The rest of the pairs with a rank greater than or equal to 0.9 is assigned to the test set. Sentences that contain more than one co-mention pair are treated as multiple individual candidates. We hand labeled five hundred to a thousand candidate sentences of each relationship type to obtain a ground truth set (Table 1)[1].

Table 1: Statistics of Candidate Sentences. We sorted each candidate sentence into a training, tuning and testing set. Numbers in parentheses show the number of positives and negatives that resulted from the hand-labeling process.

Relationship	Train	Tune	Test
Disease Associates Gene	2.35 M	31K (397+, 603-)	313K (351+, 649-)
Compound Binds Gene	1.7M	468K (37+, 463-)	227k (31+, 469-)
Compound Treats Disease	1.013M	96K (96+, 404-)	32K (112+, 388-)
Gene Interacts Gene	12.6M	1.056M (60+, 440-)	257K (76+, 424-)

Label Functions for Annotating Sentences

The challenge of having too few ground truth annotations is common to many natural language processing settings, even when unannotated text is abundant. Data programming circumvents this issue by quickly annotating large datasets by using multiple noisy signals emitted by label functions [10]. Label functions are simple pythonic functions that emit: a positive label (1), a negative label (-1) or abstain from emitting a label (0). We combine these functions using a generative model to output a single annotation, which is a consensus probability score bounded between 0 (low chance of mentioning a relationship) and 1 (high chance of mentioning a relationship). We used these annotations to train a discriminator model that makes the final classification step. Our label functions fall into three categories: databases, text patterns and domain heuristics. We provide examples for each category in our supplemental methods section.

Training Models

Generative Model

The generative model is a core part of this automatic annotation framework. It integrates multiple signals emitted by label functions and assigns a training class to each candidate sentence. This model assigns training classes by estimating the joint probability distribution of the latent true class (Y) and label function signals (Λ), $P(\Lambda, Y)$. Assuming each label function is conditionally independent, the joint distribution is defined as follows:

$$P(\Lambda, Y) = \frac{\exp(\sum_{i=1}^{m} \theta^T F_i(\Lambda, y))}{\sum_{\Lambda'} \sum_{y'} \exp(\sum_{i=1}^{m} \theta^T F_i(\Lambda', y'))}$$

where m is the number of candidate sentences, F is the vector of summary statistics and θ is a vector of weights for each summary statistic. The summary statistics used by the generative model are as follows:

$$F_{i,j}^{Lab}(\Lambda, Y) = \mathbb{1}\{\Lambda_{i,j} \neq 0\}$$
$$F_{i,j}^{Acc}(\Lambda, Y) = \mathbb{1}\{\Lambda_{i,j} = y_{i,j}\}$$

Lab is the label function's propensity (the frequency of a label function emitting a signal). *Acc* is the individual label function's accuracy given the training class. This model optimizes the weights (θ) by

minimizing the negative log likelihood:

$$\hat{\theta} = argmin_\theta - \sum_\Lambda log \sum_Y P(\Lambda, Y)$$

In the framework we used predictions from the generative model, $\hat{Y} = P(Y \mid \Lambda)$, as training classes for our dataset [67,68].

Experimental Design

Being able to re-use label functions across edge types would substantially reduce the number of label functions required to extract multiple relationships from biomedical literature. We first established a baseline by training a generative model using only distant supervision label functions designed for the target edge type. As an example, for the GiG edge type we used label functions that returned a `1` if the pair of genes were included in the Human Interaction database [69], the iRefIndex database [70] or in the Incomplete Interactome database [71]. Then we compared models that also included text and domain-heuristic label functions. Using a sampling with replacement approach, we sampled these text and domain-heuristic label functions separately within edge types, across edge types, and from a pool of all label functions. We compared within-edge-type performance to across-edge-type and all-edge-type performance. For each edge type we sampled a fixed number of label functions consisting of five evenly-spaced numbers between one and the total number of possible label functions. We repeated this sampling process 50 times for each point. We evaluated both generative and discriminative (training and downstream analyses are described in the supplemental methods section) models at each point, and we reported performance of each in terms of the area under the receiver operating characteristic curve (AUROC) and the area under the precision-recall curve (AUPR). Lastly, we conducted a follow up experiment for the generative model described in the supplemental methods section.

Results

Generative Model Using Randomly Sampled Label Functions
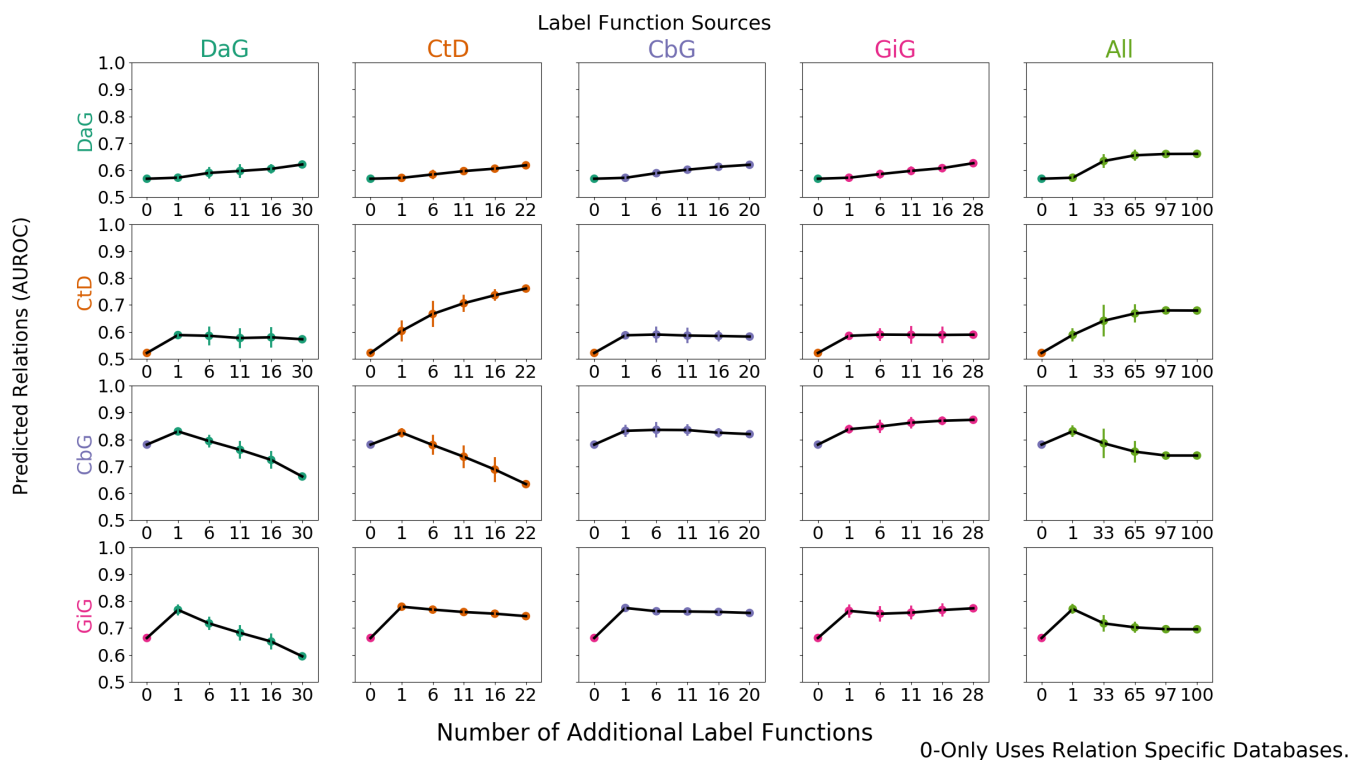
Figure 2: Grid of AUROC scores for each generative model trained on randomly sampled label functions. The rows depict the relationship each model is trying to predict and the columns are the edge type specific sources from which each label function is sampled. The right most column consists of pooling every relationship specific label function and proceeding as above.

We added randomly sampled label functions to a baseline for each edge type to evaluate the feasibility of label function re-use. Our baseline model consisted of a generative model trained with only edge-specific distant supervision label functions. We reported the results in AUROC and AUPR (Figure 2 and Supplemental Figure 5).

The on-diagonal plots of figure 2 and supplemental figure 5 show increasing performance when edge-specific label functions are added on top of the edge-specific baselines. The CtD edge type is a quintessential example of this trend. The baseline model starts off with an AUROC score of 52% and an AUPRC of 28%, which increase to 76% and 49% respectively as more CtD label functions are included. DaG edges have a similar trend: performance starting off with an AUROC of 56% and AUPR of 41% then increases to 62% and 45% respectively. Both the CbG and GiG edges have an increasing trend but plateau after a few label functions are added.

The off-diagonals in figure 2 and supplemental figure 5 show how performance varies when label functions from one edge type are added to a different edge type's baseline. In certain cases (apparent for DaG), performance increases regardless of the edge type used for label functions. In other cases (apparent with CtD), one label function appears to improve performance; however, adding more label functions does not improve performance (AUROC) or decreases it (AUPR). In certain cases, the source of the label functions appears to be important: the performance of CbG edges decrease when using label functions from the DaG and CtD categories.

Our initial hypothesis was based on the idea that certain edge types capture similar physical relationships and that these cases would be particularly amenable for label function transfer. For example, CbG and GiG both describe physical interactions. We observed that performance increased as assessed by both AUROC and AUPR when using label functions from the GiG edge type to predict CbG edges. A similar trend was observed when predicting the GiG edge; however, the performance differences were small for this edge type making the importance difficult to assess.

The last column shows increasing performance (AUROC and AUPR) for both DaG and CtD when sampling from all label functions. CbG and GiG also had increased performance when one random label function was sampled, but performance decreased drastically as more label functions were added. It is possible that a small number of irrelevant label functions are able to overwhelm the distant supervision label functions in these cases (see Figure 3 and Supplemental Figure 6).

Random Label Function Generative Model Analysis
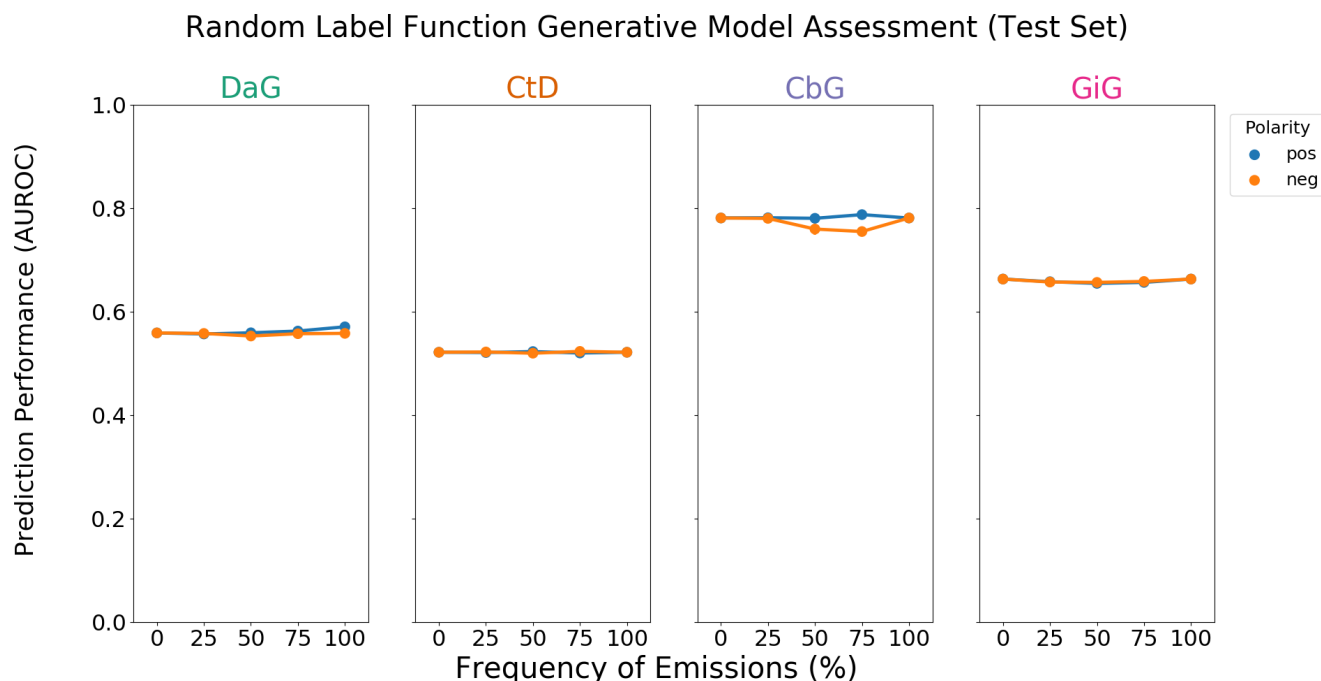
Figure 3: A grid of AUROC (A) scores for each edge type. Each plot consists of adding a single label function on top of the baseline model. This label function emits a positive (shown in blue) or negative (shown in orange) label at specified frequencies, and performance at zero is equivalent to not having a randomly emitting label function. The error bars represent 95% confidence intervals for AUROC or AUPR (y-axis) at each emission frequency.

We observed that including one label function of a mismatched type to distant supervision often improved performance, so we evaluated the effects of adding a random label function in the same setting. We found that usually adding random noise did not improve performance (Figure 3 and Supplemental Figure 6). For the CbG edge type we did observe slightly increased performance via AUPR (Supplemental Figure 6). However, performance changes in general were smaller than those observed with mismatched label types.

Discussion

We tested the feasibility of re-using label functions to extract relationships from literature. Through our sampling experiment, we found that adding relevant label functions increases prediction performance (shown in the on-diagonals of Figures 2 and Supplemental Figure 5). We found that label functions designed from relatively related edge types can increase performance (seen when GiG label functions predicts CbG and vice versa). We noticed that one edge type (DaG) is agnostic to label function source (Figure 2 and Supplemental Figure 5). Performance routinely increases when adding a single mismatched label function to our baseline model (the generative model trained only on distant supervision label functions). These results led us to hypothesize that adding a small amount of noise aided the model, but our experiment with a random label function reveals that this was not the case (Figures 3 and 6). Based on these results one question still remains: why does performance drastically increase when adding a single label function to our distant supervision baseline?

The discriminative model didn't work as intended. The majority of the time the discriminative model underperformed the generative model (Supplemental Figures [7] and [8]). Potential reasons for this are the discriminative model overfitting to the generative model's predictions and a negative class bias in some of our datasets (Table [1]). The challenges with the discriminative model are likely to have led to issues in our downstream analyses: poor model calibration (Supplemental Figure [9]) and poor recall in detecting existing Hetionet edges (Supplemental Figure [11]). Despite the above complications, our model had similar performance with a published baseline model (Supplemental Figure [10]). This implies that with better tuning the discriminative model has the potential to perform better than the baseline model.

Conclusion and Future Direction

Filling out knowledge bases via manual curation can be an arduous and erroneous task [8]. As the rate of publications increases manual curation becomes an infeasible approach. Data programming, a paradigm that uses label functions as a means to speed up the annotation process, can be used as a solution for this problem. A problem with this paradigm is that creating a useful label function takes a significant amount of time. We tested the feasibility of reusing label functions as a way to speed up the label function creation process. We conclude that label function re-use across edge types can increase performance when there are certain constraints on the number of functions re-used. More sophisticated methods of reuse may be able to capture many of the advantages and avoid many of the drawbacks. Adding more relevant label functions can increase overall performance. The discriminative model, under this paradigm, has a tendency to overfit to predictions of the generative model. We recommend implementing regularization techniques such as drop out and weight decay to combat this issue.

This work sets up the foundation for creating a common framework that mines text to create edges. Within this framework we would continuously ingest new knowledge as novel findings are published, while providing a single confidence score for an edge by consolidating sentence scores. Different from existing hetnets like Hetionet where text-derived edges generally cannot be exactly attributed to excerpts from literature [3,72], our approach would annotate each edge with its source sentences. In addition, edges generated with this approach would be unencumbered from upstream licensing or copyright restrictions, enabling openly licensed hetnets at a scale not previously possible [73,74,75]. Accordingly, we plan to use this framework to create a robust multi-edge extractor via multitask learning [68] to construct continuously updating literature-derived hetnets.

Supplemental Information

This manuscript and supplemental information are available at https://greenelab.github.io/text_mined_hetnet_manuscript/. Source code for this work is available under open licenses at: https://github.com/greenelab/snorkeling/.

Acknowledgements

References

1. **Graph Theory Enables Drug Repurposing – How a Mathematical Model Can Drive the Discovery of Hidden Mechanisms of Action**
Ruggero Gramatica, T. Di Matteo, Stefano Giorgetti, Massimo Barbiani, Dorian Bevec, Tomaso Aste
PLoS ONE (2014-01-09) https://doi.org/gf45zp
DOI: 10.1371/journal.pone.0084912 · PMID: 24416311 · PMCID: PMC3886994

2. **Drug repurposing through joint learning on knowledge graphs and literature**
Mona Alshahrani, Robert Hoehndorf
Cold Spring Harbor Laboratory (2018-08-06) https://doi.org/gf45zk
DOI: 10.1101/385617

3. **Systematic integration of biomedical knowledge prioritizes drugs for repurposing**
Daniel Scott Himmelstein, Antoine Lizee, Christine Hessler, Leo Brueggeman, Sabrina L Chen, Dexter Hadley, Ari Green, Pouya Khankhanian, Sergio E Baranzini
eLife (2017-09-22) https://doi.org/cdfk
DOI: 10.7554/elife.26726 · PMID: 28936969 · PMCID: PMC5640425

4. **Distant supervision for relation extraction without labeled data**
Mike Mintz, Steven Bills, Rion Snow, Dan Jurafsky
Proceedings of the Joint Conference of the 47th Annual Meeting of the ACL and the 4th International Joint Conference on Natural Language Processing of the AFNLP: Volume 2 - ACL-IJCNLP '09 (2009)
https://doi.org/fg9q43
DOI: 10.3115/1690219.1690287

5. **CoCoScore: Context-aware co-occurrence scoring for text mining applications using distant supervision**
Alexander Junge, Lars Juhl Jensen
Cold Spring Harbor Laboratory (2018-10-16) https://doi.org/gf45zm
DOI: 10.1101/444398

6. **Knowledge-guided convolutional networks for chemical-disease relation extraction**
Huiwei Zhou, Chengkun Lang, Zhuang Liu, Shixian Ning, Yingyu Lin, Lei Du
BMC Bioinformatics (2019-05-21) https://doi.org/gf45zn
DOI: 10.1186/s12859-019-2873-7 · PMID: 31113357 · PMCID: PMC6528333

7. **Facts from text: can text mining help to scale-up high-quality manual curation of gene products with ontologies?**
R. Winnenburg, T. Wachter, C. Plake, A. Doms, M. Schroeder
Briefings in Bioinformatics (2008-07-11) https://doi.org/bfsnwg
DOI: 10.1093/bib/bbn043 · PMID: 19060303

8. **Manual curation is not sufficient for annotation of genomic databases**
William A. Baumgartner Jr, K. Bretonnel Cohen, Lynne M. Fox, George Acquaah-Mensah, Lawrence Hunter
Bioinformatics (2007-07-01) https://doi.org/dtck86
DOI: 10.1093/bioinformatics/btm229 · PMID: 17646325 · PMCID: PMC2516305

9. **Growth rates of modern science: A bibliometric analysis based on the number of publications and cited references**
Lutz Bornmann, Rüdiger Mutz

Journal of the Association for Information Science and Technology (2015-04-29) https://doi.org/gfj5zc
DOI: 10.1002/asi.23329

10. **Data Programming: Creating Large Training Sets, Quickly**
Alexander Ratner, Christopher De Sa, Sen Wu, Daniel Selsam, Christopher Ré
arXiv (2016-05-25) https://arxiv.org/abs/1605.07723v3

11. **PKDE4J: Entity and relation extraction for public knowledge discovery.**
Min Song, Won Chul Kim, Dahee Lee, Go Eun Heo, Keun Young Kang
Journal of biomedical informatics (2015-08-12) https://www.ncbi.nlm.nih.gov/pubmed/26277115
DOI: 10.1016/j.jbi.2015.08.008 · PMID: 26277115

12. **DISEASES: Text mining and data integration of disease–gene associations**
Sune Pletscher-Frankild, Albert Pallejà, Kalliopi Tsafou, Janos X. Binder, Lars Juhl Jensen
Methods (2015-03) https://doi.org/f3mn6s
DOI: 10.1016/j.ymeth.2014.11.020 · PMID: 25484339

13. **CoCoScore: context-aware co-occurrence scoring for text mining applications using distant supervision**
Alexander Junge, Lars Juhl Jensen
Bioinformatics (2019-06-14) https://doi.org/gf4789
DOI: 10.1093/bioinformatics/btz490 · PMID: 31199464

14. **LGscore: A method to identify disease-related genes using biological literature and Google data**
Jeongwoo Kim, Hyunjin Kim, Youngmi Yoon, Sanghyun Park
Journal of Biomedical Informatics (2015-04) https://doi.org/f7bj9c
DOI: 10.1016/j.jbi.2015.01.003 · PMID: 25617670

15. **PolySearch2: a significantly improved text-mining system for discovering associations between human diseases, genes, drugs, metabolites, toxins and more**
Yifeng Liu, Yongjie Liang, David Wishart
Nucleic Acids Research (2015-04-29) https://doi.org/f7nzn5
DOI: 10.1093/nar/gkv383 · PMID: 25925572 · PMCID: PMC4489268

16. **A comprehensive and quantitative comparison of text-mining in 15 million full-text articles versus their corresponding abstracts**
David Westergaard, Hans-Henrik Stærfeldt, Christian Tønsberg, Lars Juhl Jensen, Søren Brunak
PLOS Computational Biology (2018-02-15) https://doi.org/gcx747
DOI: 10.1371/journal.pcbi.1005962 · PMID: 29447159 · PMCID: PMC5831415

17. **The research on gene-disease association based on text-mining of PubMed**
Jie Zhou, Bo-quan Fu
BMC Bioinformatics (2018-02-07) https://doi.org/gf479k
DOI: 10.1186/s12859-018-2048-y · PMID: 29415654 · PMCID: PMC5804013

18. **A global network of biomedical relationships derived from text**
Bethany Percha, Russ B Altman
Bioinformatics (2018-02-27) https://doi.org/gc3ndk
DOI: 10.1093/bioinformatics/bty114 · PMID: 29490008 · PMCID: PMC6061699

19. **Literature mining for the biologist: from information retrieval to biological discovery**
Lars Juhl Jensen, Jasmin Saric, Peer Bork

Nature Reviews Genetics (2006-02) https://doi.org/bgq7q9
DOI: 10.1038/nrg1768 · PMID: 16418747

20. **Application of text mining in the biomedical domain**
Wilco W. M. Fleuren, Wynand Alkema
Methods (2015-03) https://doi.org/f64p6n
DOI: 10.1016/j.ymeth.2015.01.015 · PMID: 25641519

21. **Extraction of relations between genes and diseases from text and large-scale data analysis: implications for translational research**
Àlex Bravo, Janet Piñero, Núria Queralt-Rosinach, Michael Rautschka, Laura I Furlong
BMC Bioinformatics (2015-02-21) https://doi.org/f7kn8s
DOI: 10.1186/s12859-015-0472-9 · PMID: 25886734 · PMCID: PMC4466840

22. **The EU-ADR corpus: Annotated drugs, diseases, targets, and their relationships**
Erik M. van Mulligen, Annie Fourrier-Reglat, David Gurwitz, Mariam Molokhia, Ainhoa Nieto, Gianluca Trifiro, Jan A. Kors, Laura I. Furlong
Journal of Biomedical Informatics (2012-10) https://doi.org/f36vn6
DOI: 10.1016/j.jbi.2012.04.004 · PMID: 22554700

23. **CoMAGC: a corpus with multi-faceted annotations of gene-cancer relations**
Hee-Jin Lee, Sang-Hyung Shim, Mi-Ryoung Song, Hyunju Lee, Jong C Park
BMC Bioinformatics (2013) https://doi.org/gb8v5s
DOI: 10.1186/1471-2105-14-323 · PMID: 24225062 · PMCID: PMC3833657

24. **Concept annotation in the CRAFT corpus**
Michael Bada, Miriam Eckert, Donald Evans, Kristin Garcia, Krista Shipley, Dmitry Sitnikov, William A Baumgartner, K Bretonnel Cohen, Karin Verspoor, Judith A Blake, Lawrence E Hunter
BMC Bioinformatics (2012-07-09) https://doi.org/gb8vdr
DOI: 10.1186/1471-2105-13-161 · PMID: 22776079 · PMCID: PMC3476437

25. **DTMiner: identification of potential disease targets through biomedical literature mining**
Dong Xu, Meizhuo Zhang, Yanping Xie, Fan Wang, Ming Chen, Kenny Q. Zhu, Jia Wei
Bioinformatics (2016-08-09) https://doi.org/f9nw36
DOI: 10.1093/bioinformatics/btw503 · PMID: 27506226 · PMCID: PMC5181534

26. **Automatic extraction of gene-disease associations from literature using joint ensemble learning**
Balu Bhasuran, Jeyakumar Natarajan
PLOS ONE (2018-07-26) https://doi.org/gdx63f
DOI: 10.1371/journal.pone.0200699 · PMID: 30048465 · PMCID: PMC6061985

27. **BioBERT: a pre-trained biomedical language representation model for biomedical text mining**
Jinhyuk Lee, Wonjin Yoon, Sungdong Kim, Donghyeon Kim, Sunkyu Kim, Chan Ho So, Jaewoo Kang
arXiv (2019-01-25) https://arxiv.org/abs/1901.08746v3

28. **Distant Supervision for Large-Scale Extraction of Gene–Disease Associations from Literature Using DeepDive**
Balu Bhasuran, Jeyakumar Natarajan
International Conference on Innovative Computing and Communications (2018-11-20)
https://doi.org/gf5hfv
DOI: 10.1007/978-981-13-2354-6_39

29. **A new method for prioritizing drug repositioning candidates extracted by literature-based discovery**
Majid Rastegar-Mojarad, Ravikumar Komandur Elayavilli, Dingcheng Li, Rashmi Prasad, Hongfang Liu
2015 IEEE International Conference on Bioinformatics and Biomedicine (BIBM) (2015-11)
https://doi.org/gf479j
DOI: 10.1109/bibm.2015.7359766

30. **Literature Mining for the Discovery of Hidden Connections between Drugs, Genes and Diseases**
Raoul Frijters, Marianne van Vugt, Ruben Smeets, René van Schaik, Jacob de Vlieg, Wynand Alkema
PLoS Computational Biology (2010-09-23) https://doi.org/bhrw7x
DOI: 10.1371/journal.pcbi.1000943 · PMID: 20885778 · PMCID: PMC2944780

31. **Large-scale extraction of accurate drug-disease treatment pairs from biomedical literature for drug repurposing**
Rong Xu, QuanQiu Wang
BMC Bioinformatics (2013-06-06) https://doi.org/gb8v3k
DOI: 10.1186/1471-2105-14-181 · PMID: 23742147 · PMCID: PMC3702428

32. **BioCreative V CDR task corpus: a resource for chemical disease relation extraction**
Jiao Li, Yueping Sun, Robin J. Johnson, Daniela Sciaky, Chih-Hsuan Wei, Robert Leaman, Allan Peter Davis, Carolyn J. Mattingly, Thomas C. Wiegers, Zhiyong Lu
Database (2016) https://doi.org/gf5hfw
DOI: 10.1093/database/baw068 · PMID: 27161011 · PMCID: PMC4860626

33. **Overview of the biocreative vi chemical-protein interaction track**
Martin Krallinger, Obdulia Rabal, Saber A Akhondi, others
Proceedings of the sixth biocreative challenge evaluation workshop (2017)
https://www.semanticscholar.org/paper/Overview-of-the-BioCreative-VI-chemical-protein-Krallinger-Rabal/eed781f498b563df5a9e8a241c67d63dd1d92ad5

34. **LimTox: a web tool for applied text mining of adverse event and toxicity associations of compounds, drugs and genes**
Andres Cañada, Salvador Capella-Gutierrez, Obdulia Rabal, Julen Oyarzabal, Alfonso Valencia, Martin Krallinger
Nucleic Acids Research (2017-05-22) https://doi.org/gf479h
DOI: 10.1093/nar/gkx462 · PMID: 28531339 · PMCID: PMC5570141

35. **LPTK: a linguistic pattern-aware dependency tree kernel approach for the BioCreative VI CHEMPROT task**
Neha Warikoo, Yung-Chun Chang, Wen-Lian Hsu
Database (2018-01-01) https://doi.org/gfhjr6
DOI: 10.1093/database/bay108 · PMID: 30346607 · PMCID: PMC6196310

36. **Extracting chemical–protein relations with ensembles of SVM and deep learning models**
Yifan Peng, Anthony Rios, Ramakanth Kavuluru, Zhiyong Lu
Database (2018-01-01) https://doi.org/gf479f
DOI: 10.1093/database/bay073 · PMID: 30020437 · PMCID: PMC6051439

37. **Extracting chemical–protein interactions from literature using sentence structure analysis and feature engineering**
Pei-Yau Lung, Zhe He, Tingting Zhao, Disa Yu, Jinfeng Zhang

Database (2019-01-01) https://doi.org/gf479g
DOI: 10.1093/database/bay138 · PMID: 30624652 · PMCID: PMC6323317

38. **Improving the learning of chemical-protein interactions from literature using transfer learning and specialized word embeddings**
P Corbett, J Boyle
Database (2018-01-01) https://doi.org/gf479d
DOI: 10.1093/database/bay066 · PMID: 30010749 · PMCID: PMC6044291

39. **Extracting chemical–protein relations using attention-based neural networks**
Sijia Liu, Feichen Shen, Ravikumar Komandur Elayavilli, Yanshan Wang, Majid Rastegar-Mojarad, Vipin Chaudhary, Hongfang Liu
Database (2018-01-01) https://doi.org/gfdz8d
DOI: 10.1093/database/bay102 · PMID: 30295724 · PMCID: PMC6174551

40. **Chemical–gene relation extraction using recursive neural network**
Sangrak Lim, Jaewoo Kang
Database (2018-01-01) https://doi.org/gdss6f
DOI: 10.1093/database/bay060 · PMID: 29961818 · PMCID: PMC6014134

41. **Exploring Semi-supervised Variational Autoencoders for Biomedical Relation Extraction**
Yijia Zhang, Zhiyong Lu
arXiv (2019-01-18) https://arxiv.org/abs/1901.06103v1

42. **Pharmspresso: a text mining tool for extraction of pharmacogenomic concepts and relationships from full text**
Yael Garten, Russ B Altman
BMC Bioinformatics (2009-02) https://doi.org/df75hq
DOI: 10.1186/1471-2105-10-s2-s6 · PMID: 19208194 · PMCID: PMC2646239

43. **STRING v10: protein–protein interaction networks, integrated over the tree of life**
Damian Szklarczyk, Andrea Franceschini, Stefan Wyder, Kristoffer Forslund, Davide Heller, Jaime Huerta-Cepas, Milan Simonovic, Alexander Roth, Alberto Santos, Kalliopi P. Tsafou, … Christian von Mering
Nucleic Acids Research (2014-10-28) https://doi.org/f64rfn
DOI: 10.1093/nar/gku1003 · PMID: 25352553 · PMCID: PMC4383874

44. **PPInterFinder—a mining tool for extracting causal relations on human proteins from literature**
Kalpana Raja, Suresh Subramani, Jeyakumar Natarajan
Database (2013-01-01) https://doi.org/gf479b
DOI: 10.1093/database/bas052 · PMID: 23325628 · PMCID: PMC3548331

45. **HPIminer: A text mining system for building and visualizing human protein interaction networks and pathways**
Suresh Subramani, Raja Kalpana, Pankaj Moses Monickaraj, Jeyakumar Natarajan
Journal of Biomedical Informatics (2015-04) https://doi.org/f7bgnr
DOI: 10.1016/j.jbi.2015.01.006 · PMID: 25659452

46. **Analyzing a co-occurrence gene-interaction network to identify disease-gene association**
Amira Al-Aamri, Kamal Taha, Yousof Al-Hammadi, Maher Maalouf, Dirar Homouz
BMC Bioinformatics (2019-02-08) https://doi.org/gf49nm
DOI: 10.1186/s12859-019-2634-7 · PMID: 30736752 · PMCID: PMC6368766

47. **Comparative experiments on learning information extractors for proteins and their interactions**
Razvan Bunescu, Ruifang Ge, Rohit J. Kate, Edward M. Marcotte, Raymond J. Mooney, Arun K. Ramani, Yuk Wah Wong
Artificial Intelligence in Medicine (2005-02) https://doi.org/dhztpn
DOI: 10.1016/j.artmed.2004.07.016 · PMID: 15811782

48. **BioInfer: a corpus for information extraction in the biomedical domain**
Sampo Pyysalo, Filip Ginter, Juho Heimonen, Jari Björne, Jorma Boberg, Jouni Järvinen, Tapio Salakoski
BMC Bioinformatics (2007-02-09) https://doi.org/b7bhhc
DOI: 10.1186/1471-2105-8-50 · PMID: 17291334 · PMCID: PMC1808065

49. **Learning language in logic - genic interaction extraction challenge**
C. Nédellec
Proceedings of the learning language in logic 2005 workshop at the international conference on machine learning (2005)

50. **RelEx–Relation extraction using dependency parse trees**
K. Fundel, R. Kuffner, R. Zimmer
Bioinformatics (2006-12-01) https://doi.org/cz7q4d
DOI: 10.1093/bioinformatics/btl616 · PMID: 17142812

51. **Mining medline: Abstracts, sentences, or phrases?**
Jing Ding, Daniel Berleant, Dan Nettleton, Eve Syrkin Wurtele
Pacific symposium on biocomputing (2002) http://helix-web.stanford.edu/psb02/ding.pdf

52. **Comparative analysis of five protein-protein interaction corpora**
Sampo Pyysalo, Antti Airola, Juho Heimonen, Jari Björne, Filip Ginter, Tapio Salakoski
BMC Bioinformatics (2008-04) https://doi.org/fh3df7
DOI: 10.1186/1471-2105-9-s3-s6 · PMID: 18426551 · PMCID: PMC2349296

53. **Exploiting graph kernels for high performance biomedical relation extraction**
Nagesh C. Panyam, Karin Verspoor, Trevor Cohn, Kotagiri Ramamohanarao
Journal of Biomedical Semantics (2018-01-30) https://doi.org/gf49nn
DOI: 10.1186/s13326-017-0168-3 · PMID: 29382397 · PMCID: PMC5791373

54. **Text Mining for Protein Docking**
Varsha D. Badal, Petras J. Kundrotas, Ilya A. Vakser
PLOS Computational Biology (2015-12-09) https://doi.org/gcvj3b
DOI: 10.1371/journal.pcbi.1004630 · PMID: 26650466 · PMCID: PMC4674139

55. **Feature assisted stacked attentive shortest dependency path based Bi-LSTM model for protein–protein interaction**
Shweta Yadav, Asif Ekbal, Sriparna Saha, Ankit Kumar, Pushpak Bhattacharyya
Knowledge-Based Systems (2019-02) https://doi.org/gf4788
DOI: 10.1016/j.knosys.2018.11.020

56. **Extraction of protein–protein interactions (PPIs) from the literature by deep convolutional neural networks with various feature embeddings**
Sung-Pil Choi
Journal of Information Science (2016-11) https://doi.org/gcv8bn
DOI: 10.1177/0165551516673485

57. **Deep learning for extracting protein-protein interactions from biomedical literature**
Yifan Peng, Zhiyong Lu
arXiv (2017-06-05) https://arxiv.org/abs/1706.01556v2

58. **Large-scale extraction of gene interactions from full-text literature using DeepDive**
Emily K. Mallory, Ce Zhang, Christopher Ré, Russ B. Altman
Bioinformatics (2015-09-03) https://doi.org/gb5g7b
DOI: 10.1093/bioinformatics/btv476 · PMID: 26338771 · PMCID: PMC4681986

59. **The new NHGRI-EBI Catalog of published genome-wide association studies (GWAS Catalog)**
Jacqueline MacArthur, Emily Bowler, Maria Cerezo, Laurent Gil, Peggy Hall, Emma Hastings, Heather Junkins, Aoife McMahon, Annalisa Milano, Joannella Morales, ... Helen Parkinson
Nucleic Acids Research (2016-11-29) https://doi.org/f9v7cp
DOI: 10.1093/nar/gkw1133 · PMID: 27899670 · PMCID: PMC5210590

60. **DrugBank 5.0: a major update to the DrugBank database for 2018**
David S Wishart, Yannick D Feunang, An C Guo, Elvis J Lo, Ana Marcu, Jason R Grant, Tanvir Sajed, Daniel Johnson, Carin Li, Zinat Sayeeda, ... Michael Wilson
Nucleic Acids Research (2017-11-08) https://doi.org/gcwtzk
DOI: 10.1093/nar/gkx1037 · PMID: 29126136 · PMCID: PMC5753335

61. **PubTator: a web-based text mining tool for assisting biocuration**
Chih-Hsuan Wei, Hung-Yu Kao, Zhiyong Lu
Nucleic Acids Research (2013-05-22) https://doi.org/f475th
DOI: 10.1093/nar/gkt441 · PMID: 23703206 · PMCID: PMC3692066

62. **DNorm: disease name normalization with pairwise learning to rank**
R. Leaman, R. Islamaj Dogan, Z. Lu
Bioinformatics (2013-08-21) https://doi.org/f5gj9n
DOI: 10.1093/bioinformatics/btt474 · PMID: 23969135 · PMCID: PMC3810844

63. **GeneTUKit: a software for document-level gene normalization**
M. Huang, J. Liu, X. Zhu
Bioinformatics (2011-02-08) https://doi.org/dng2cb
DOI: 10.1093/bioinformatics/btr042 · PMID: 21303863 · PMCID: PMC3065680

64. **Cross-species gene normalization by species inference**
Chih-Hsuan Wei, Hung-Yu Kao
BMC Bioinformatics (2011-10-03) https://doi.org/dnmvds
DOI: 10.1186/1471-2105-12-s8-s5 · PMID: 22151999 · PMCID: PMC3269940

65. **Collaborative biocuration–text-mining development task for document prioritization for curation**
T. C. Wiegers, A. P. Davis, C. J. Mattingly
Database (2012-11-22) https://doi.org/gbb3zw
DOI: 10.1093/database/bas037 · PMID: 23180769 · PMCID: PMC3504477

66. **The Stanford CoreNLP Natural Language Processing Toolkit**
Christopher Manning, Mihai Surdeanu, John Bauer, Jenny Finkel, Steven Bethard, David McClosky
Proceedings of 52nd Annual Meeting of the Association for Computational Linguistics: System Demonstrations (2014) https://doi.org/gf3xhp
DOI: 10.3115/v1/p14-5010

67. **Snorkel**
Alexander Ratner, Stephen H. Bach, Henry Ehrenberg, Jason Fries, Sen Wu, Christopher Ré
Proceedings of the VLDB Endowment (2017-11-01) https://doi.org/ch44
DOI: 10.14778/3157794.3157797 · PMID: 29770249 · PMCID: PMC5951191

68. **Snorkel MeTaL**
Alex Ratner, Braden Hancock, Jared Dunnmon, Roger Goldman, Christopher Ré
Proceedings of the Second Workshop on Data Management for End-To-End Machine Learning - DEEM'18 (2018) https://doi.org/gf3xk7
DOI: 10.1145/3209889.3209898 · PMID: 30931438 · PMCID: PMC6436830

69. **A Proteome-Scale Map of the Human Interactome Network**
Thomas Rolland, Murat Taşan, Benoit Charloteaux, Samuel J. Pevzner, Quan Zhong, Nidhi Sahni, Song Yi, Irma Lemmens, Celia Fontanillo, Roberto Mosca, … Marc Vidal
Cell (2014-11) https://doi.org/f3mn6x
DOI: 10.1016/j.cell.2014.10.050 · PMID: 25416956 · PMCID: PMC4266588

70. **iRefIndex: A consolidated protein interaction database with provenance**
Sabry Razick, George Magklaras, Ian M Donaldson
BMC Bioinformatics (2008) https://doi.org/b99bjj
DOI: 10.1186/1471-2105-9-405 · PMID: 18823568 · PMCID: PMC2573892

71. **Uncovering disease-disease relationships through the incomplete interactome**
J. Menche, A. Sharma, M. Kitsak, S. D. Ghiassian, M. Vidal, J. Loscalzo, A.-L. Barabasi
Science (2015-02-19) https://doi.org/f3mn6z
DOI: 10.1126/science.1257601 · PMID: 25700523 · PMCID: PMC4435741

72. **Mining knowledge from MEDLINE articles and their indexed MeSH terms**
Daniel Himmelstein, Alex Pankov
ThinkLab (2015-05-10) https://doi.org/f3mqwp
DOI: 10.15363/thinklab.d67

73. **Integrating resources with disparate licensing into an open network**
Daniel Himmelstein, Lars Juhl Jensen, MacKenzie Smith, Katie Fortney, Caty Chung
ThinkLab (2015-08-28) https://doi.org/bfmk
DOI: 10.15363/thinklab.d107

74. **Legal confusion threatens to slow data science**
Simon Oxenham
Nature (2016-08) https://doi.org/bndt
DOI: 10.1038/536016a · PMID: 27488781

75. **An analysis and metric of reusable data licensing practices for biomedical resources**
Seth Carbon, Robin Champieux, Julie A. McMurry, Lilly Winfree, Letisha R. Wyatt, Melissa A. Haendel
PLOS ONE (2019-03-27) https://doi.org/gf5m8v
DOI: 10.1371/journal.pone.0213090 · PMID: 30917137 · PMCID: PMC6436688

76. **A Sensitivity Analysis of (and Practitioners' Guide to) Convolutional Neural Networks for Sentence Classification**
Ye Zhang, Byron Wallace
arXiv (2015-10-13) https://arxiv.org/abs/1510.03820v4

77. **Adam: A Method for Stochastic Optimization**
Diederik P. Kingma, Jimmy Ba
arXiv (2014-12-22) https://arxiv.org/abs/1412.6980v9

78. **Distributed Representations of Words and Phrases and their Compositionality**
Tomas Mikolov, Ilya Sutskever, Kai Chen, Greg Corrado, Jeffrey Dean
arXiv (2013-10-16) https://arxiv.org/abs/1310.4546v1

79. **Enriching Word Vectors with Subword Information**
Piotr Bojanowski, Edouard Grave, Armand Joulin, Tomas Mikolov
arXiv (2016-07-15) https://arxiv.org/abs/1607.04606v2

80. **Efficient Estimation of Word Representations in Vector Space**
Tomas Mikolov, Kai Chen, Greg Corrado, Jeffrey Dean
arXiv (2013-01-16) https://arxiv.org/abs/1301.3781v3

81. **On Calibration of Modern Neural Networks**
Chuan Guo, Geoff Pleiss, Yu Sun, Kilian Q. Weinberger
arXiv (2017-06-14) https://arxiv.org/abs/1706.04599v2

82. **Accurate Uncertainties for Deep Learning Using Calibrated Regression**
Volodymyr Kuleshov, Nathan Fenner, Stefano Ermon
arXiv (2018-07-01) https://arxiv.org/abs/1807.00263v1

Supplemental Methods

Label Function Categories

We provide examples of label function categories below. Each example regards the following candidate sentence: "PTK6 may be a novel therapeutic target for pancreatic cancer."

Databases: These label functions incorporate existing databases to generate a signal, as seen in distant supervision [4]. These functions detect if a candidate sentence's co-mention pair is present in a given database. If the candidate pair is present, our label function emitted a positive label and abstained otherwise. If the candidate pair wasn't present in any existing database, a separate label function emitted a negative label. We used a separate label function to prevent a label imbalance problem that we encountered during development: emitting positive and negatives from the same label functions appeared to result in classifiers that predict almost exclusively negative predictions.

$$\Lambda_{DB}(D, G) = \begin{cases} 1 & (D, G) \in DB \\ 0 & otherwise \end{cases}$$

$$\Lambda_{\neg DB}(D, G) = \begin{cases} -1 & (D, G) \notin DB \\ 0 & otherwise \end{cases}$$

Text Patterns: These label functions are designed to use keywords and sentence context to generate a signal. For example, a label function could focus on the number of words between two mentions or focus on the grammatical structure of a sentence. These functions emit a positive or negative label depending on the situation.

$$\Lambda_{TP}(D, G) = \begin{cases} 1 & "\,target\," \in Candidate\ Sentence \\ 0 & otherwise \end{cases}$$

$$\Lambda_{TP}(D, G) = \begin{cases} -1 & "\,VB\," \notin pos\_tags(Candidate\ Sentence) \\ 0 & otherwise \end{cases}$$

Domain Heuristics: These label functions use the other experiment results to generate a signal. For this category, we used dependency path cluster themes generated by Percha et al. [18]. If a candidate sentence's dependency path belongs to a previously generated cluster, then the label function will emit a positive label and abstain otherwise.

$$\Lambda_{DH}(D, G) = \begin{cases} 1 & Candidate\ Sentence \in Cluster\ Theme \\ 0 & otherwise \end{cases}$$

Roughly half of our label functions are based on text patterns, while the others are distributed across the databases and domain heuristics (Table 2).

Table 2: The distribution of each label function per relationship.

Relationship	Databases (DB)	Text Patterns (TP)	Domain Heuristics (DH)
DaG	7	20	10
CtD	3	15	7
CbG	9	13	7

Relationship	Databases (DB)	Text Patterns (TP)	Domain Heuristics (DH)
GiG	9	20	8

Adding Random Noise to Generative Model

We discovered in the course of this work that adding a single label function from a mismatched type would often improve the performance of the generative model (see Results). We designed an experiment to test whether adding a noisy label function also increased performance. This label function emitted a positive or negative label at varying frequencies, which were evenly spaced from zero to one. Zero was the same as distant supervision and one meant that all sentences were randomly labeled. We trained the generative model with these label functions added and reported results in terms of AUROC and AUPR.

Discriminative Model

The discriminative model is a neural network, which we train to predict labels from the generative model. The expectation is that the discriminative model can learn more complete features of the text than the label functions used in the generative model. We used a convolutional neural network with multiple filters as our discriminative model. This network uses multiple filters with fixed widths of 300 dimensions and a fixed height of 7 (Figure 4), because this height provided the best performance in terms of relationship classification [76]. We trained this model for 20 epochs using the adam optimizer [77] with pytorch's default parameter settings and a learning rate of 0.001. We added a L2 penalty on the network weights to prevent overfitting. Lastly, we added a dropout layer (p=0.25) between the fully connected layer and the softmax layer.
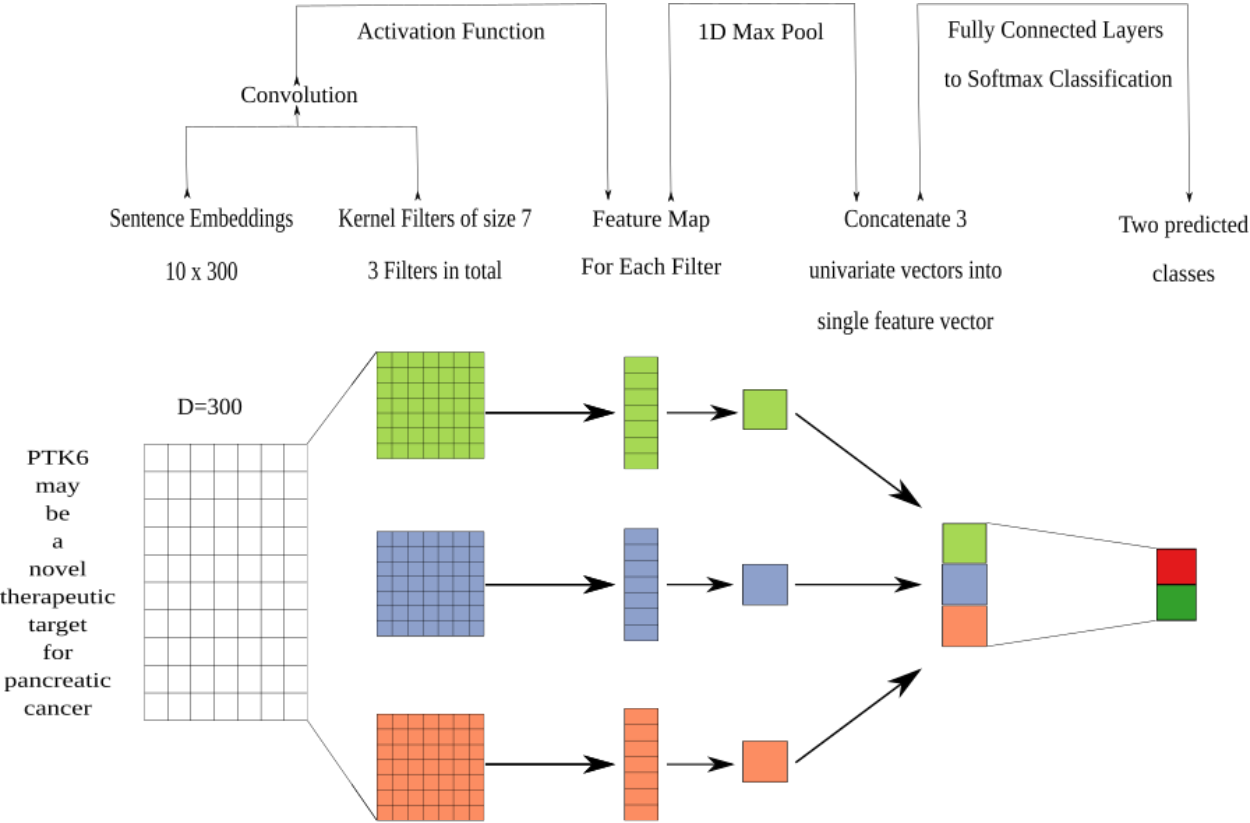
Figure 4: The architecture of the discriminative model was a convolutional neural network. We performed a convolution step using multiple filters. The filters generated a feature map that was sent into a maximum pooling layer that was designed to extract the largest feature in each map. The extracted features were concatenated into a singular vector that was passed into a fully connected network. The fully connected network had 300 neurons for the first layer, 100 neurons for the second layer and 50 neurons for the last layer. The last step from the fully connected network was to generate predictions using a softmax layer.

Word Embeddings

Word embeddings are representations that map individual words to real valued vectors of user-specified dimensions. These embeddings have been shown to capture the semantic and syntactic information between words [78]. We trained Facebook's fastText [79] using all candidate sentences for each individual relationship pair to generate word embeddings. fastText uses a skipgram model [80] that aims to predict the surrounding context for a candidate word and pairs the model with a novel scoring function that treats each word as a bag of character n-grams. We trained this model for 20 epochs using a window size of 2 and generated 300-dimensional word embeddings. We use the optimized word embeddings to train a discriminative model.

Calibration of the Discriminative Model

Often many tasks require a machine learning model to output reliable probability predictions. A model is well calibrated if the probabilities emitted from the model match the observed probabilities: a well-calibrated model that assigns a class label with 80% probability should have that class appear 80% of the time. Deep neural network models can often be poorly calibrated [81,82]. These models are usually over-confident in their predictions. As a result, we calibrated our convolutional neural network using temperature scaling. Temperature scaling uses a parameter T to scale each value of the logit vector (z) before being passed into the softmax (SM) function.

$$\sigma_{SM}\left(\frac{z_i}{T}\right) = \frac{\exp\left(\frac{z_i}{T}\right)}{\sum_i \exp\left(\frac{z_i}{T}\right)}$$

We found the optimal T by minimizing the negative log likelihood (NLL) of a held out validation set. The benefit of using this method is that the model becomes more reliable and the accuracy of the model doesn't change [81].

Supplemental Tables and Figures

Generative Model AUPR Performance

Figure 5: Grid of AUPR scores for each generative model trained on randomly sampled label functions. The rows depict the relationship each model is trying to predict and the columns are the edge type specific sources from which each label function is sampled. For example, the top-left most square depicts the generative model predicting DaG sentences, while randomly sampling label functions designed to predict the DaG relationship. The square towards the right depicts the generative model predicting DaG sentences, while randomly sampling label functions designed to predict the CtD relationship. This pattern continues filling out the rest of the grid. The right most column consists of pooling every relationship specific label function and proceeding as above.

Random Label Function Generative Model Analysis

Figure 6: A grid of AUROC (A) scores for each edge type. Each plot consists of adding a single label function on top of the baseline model. This label function emits a positive (shown in blue) or negative (shown in orange) label at specified frequencies, and performance at zero is equivalent to not having a randomly emitting label function. The error bars represent 95% confidence intervals for AUROC or AUPR (y-axis) at each emission frequency.

Discriminative Model Performance

Label Sampling Discriminator Model Assessment (Test Set)
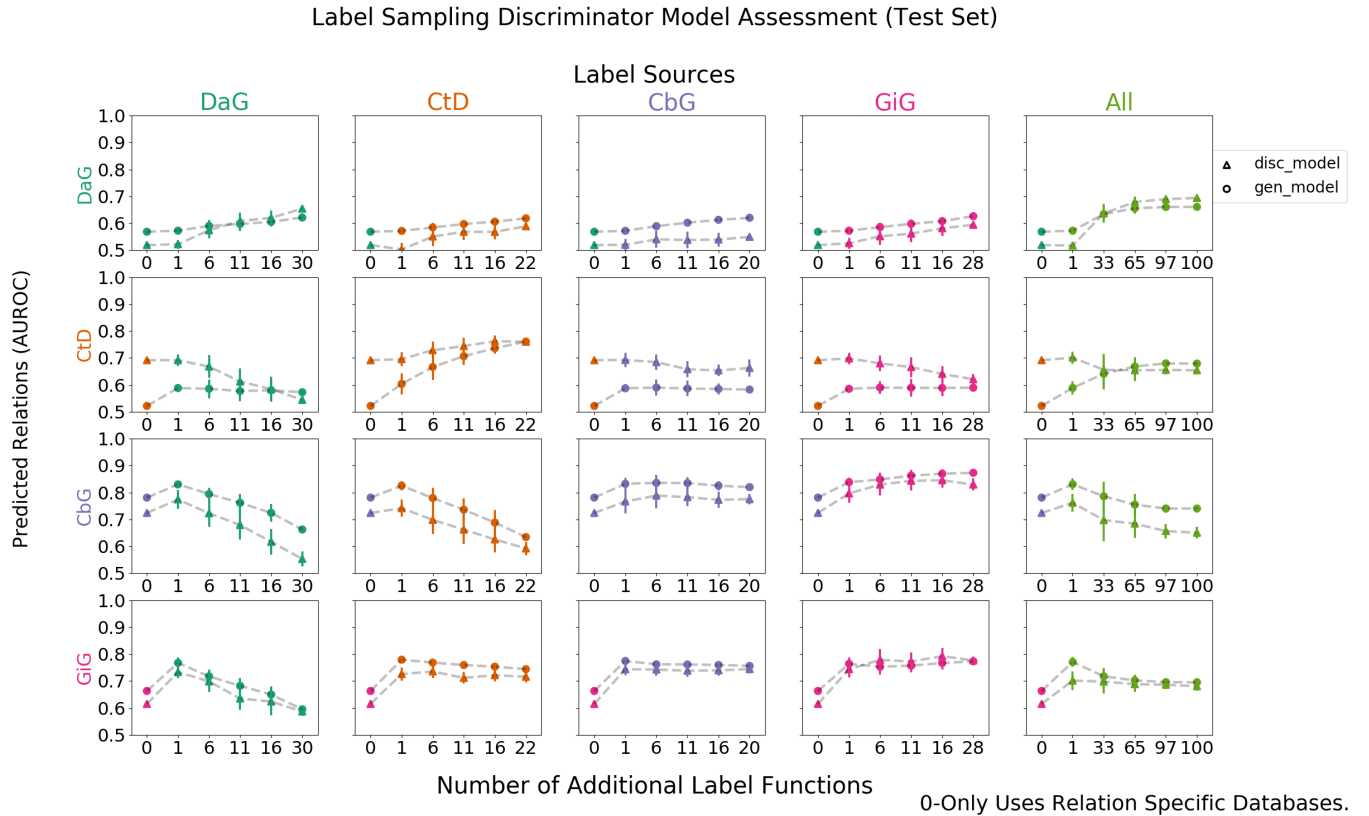
Figure 7: Grid of AUROC scores for each discriminative model trained using generated labels from the generative models. The rows depict the edge type each model is trying to predict and the columns are the edge type specific sources from which each label function was sampled. For example, the top-left most square depicts the discriminator model predicting DaG sentences, while randomly sampling label functions designed to predict the DaG relationship. The error bars over the points represents the standard deviation between sampled runs. The square towards the right depicts the discriminative model predicting DaG sentences, while randomly sampling label functions designed to predict the CtD relationship. This pattern continues filling out the rest of the grid. The right most column consists of pooling every relationship specific label function and proceeding as above.

In this framework we used a generative model trained over label functions to produce probabilistic training labels for each sentence. Then we trained a discriminative model, which has full access to a representation of the text of the sentence, to predict the generated labels. The discriminative model is a convolutional neural network trained over word embeddings (See Methods). We report the results of the discriminative model using AUROC and AUPR (Figures 7 and 8).

We found that the discriminative model under-performed the generative model in most cases. Only for the CtD edge does the discriminative model appear to provide performance above the generative model and that increased performance is only with a modest number of label functions. With the full set of label functions, performance of both models remain similar. The one or a few mismatched label functions (off-diagonal) improving generative model performance trend is retained despite the limited performance of the discriminative model.
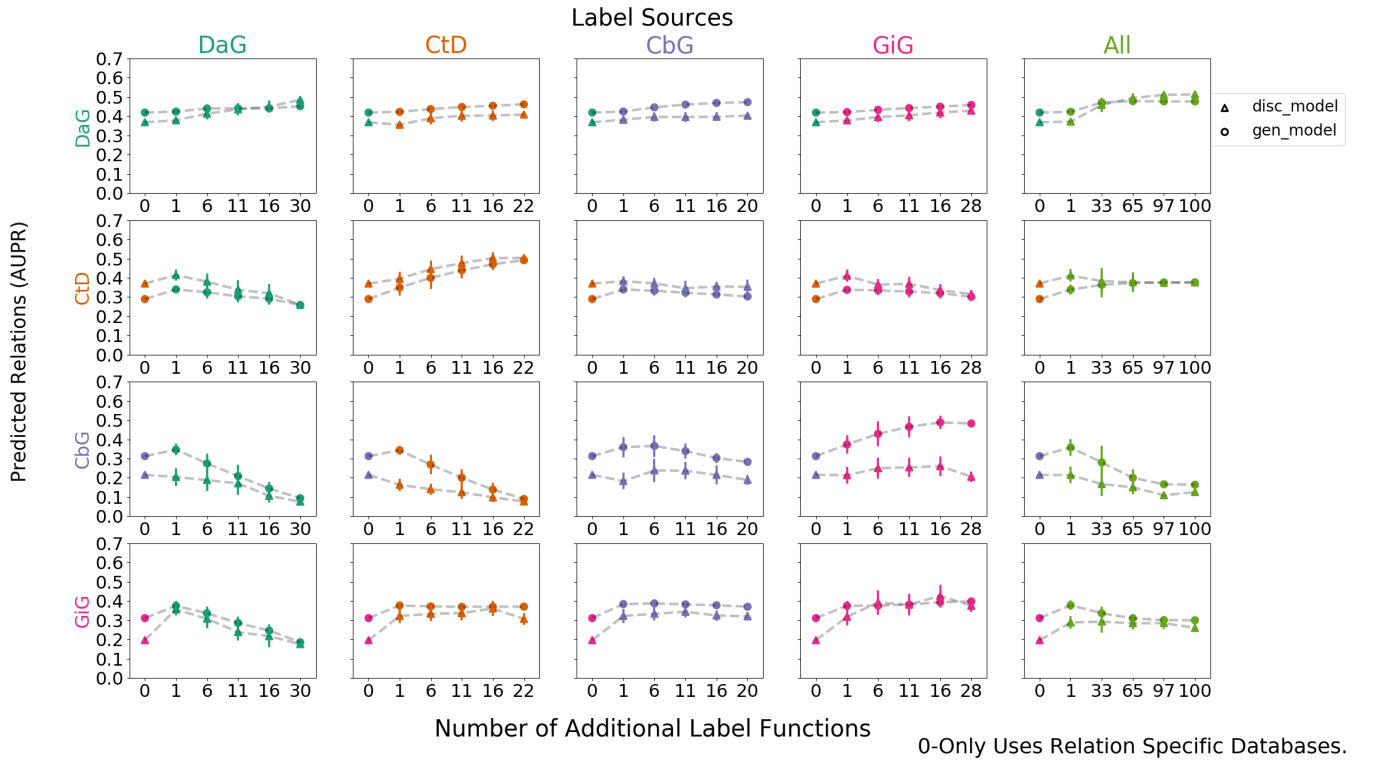
Figure 8: Grid of AUPR scores for each discriminative model trained using generated labels from the generative models. The rows depict the edge type each model is trying to predict and the columns are the edge type specific sources from which each label function was sampled. For example, the top-left most square depicts the discriminator model predicting DaG sentences, while randomly sampling label functions designed to predict the DaG relationship. The error bars over the points represents the standard deviation between sampled runs. The square towards the right depicts the discriminative model predicting DaG sentences, while randomly sampling label functions designed to predict the CtD relationship. This pattern continues filling out the rest of the grid. The right most column consists of pooling every relationship specific label function and proceeding as above.

Discriminative Model Calibration
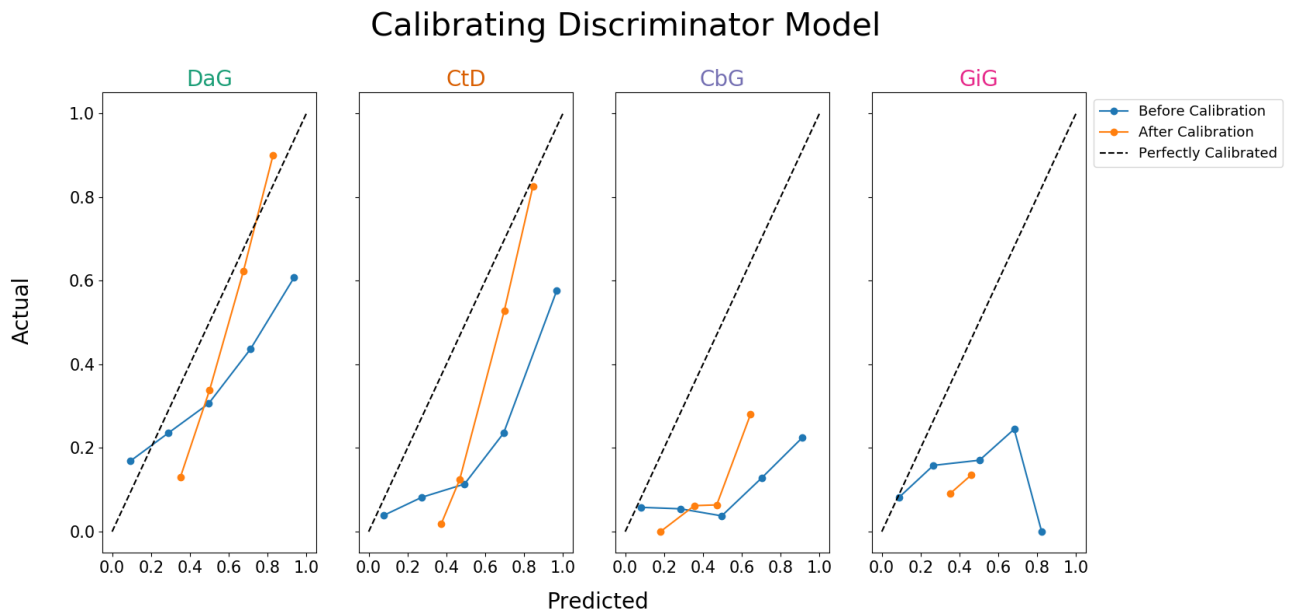
Figure 9: Calibration plots for the discriminative model. A perfectly calibrated model would follow the dashed diagonal line. The blue line represents the predictions before calibration and the orange line shows predictions after calibration.

Even deep learning models with high precision and recall can be poorly calibrated, and the overconfidence of these models has been noted [81,82]. We attempted to calibrate the best performing discriminative model so that we could directly use the emitted probabilities. We examined the calibration of our existing model (Supplemental Figure 9, blue line). We found that the DaG and CtG edge types were, though not perfectly calibrated, were somewhat aligned with the ideal calibration lines. The CbG and GiG edges were poorly calibrated and increasing model certainty did not always lead to an increase in precision. Applying the calibration algorithm (orange line) did not appear to bring predictions in line with the ideal calibration line, but did capture some of the uncertainty in the GiG edge type. For this reason we use the measured precision instead of the predicted probabilities when determining how many edges could be added to existing knowledge bases with specified levels of confidence.

Model Calibration Tables

Table 3: Contains the top ten Disease-associates-Gene confidence scores before and after model calbration. Disease mentions are highlighted in brown and Gene mentions are highlighted in blue.

Disease Name	Gene Symbol	Text	Before Calibration	After Calibraiton
adrenal gland cancer	TP53	the mechanisms of adrenal tumorigenesis remain poorly established ; the r337h germline mutation in the p53 gene has previously been associated with acts in brazilian children .	1.0	0.882
breast cancer	ERBB2	in breast cancer , overexpression of her2 is associated with an aggressive tumor phenotype and poor prognosis .	1.0	0.845
lung cancer	TP53	however , both adenine (a) and guanine (g) mutations are found in the p53 gene in cr exposure-related lung cancer .	1.0	0.83
malignant glioma	BAX	these data suggest that the combination of tra-8 treatment with specific overexpression of bax using advegfbax may be an effective approach for the treatment of human malignant gliomas .	0.999	0.827
polycystic ovary syndrome	SERPINE1	4 g allele in pai-1 gene was more frequent in pcos and the 4g/4 g genotype was associated with increased pai-1 levels .	0.999	0.814
systemic lupus erythematosus	PRL	results : sle patients showed a significantly higher serum level of prl than healthy subjects , which was especially obvious in the active stage of the disease (p = 0.000 .	0.999	0.813
hematologic cancer	TNF	the mean tnf-alpha plasma concentration in the patients with cll was significantly higher than in the healthy control population (16.4 versus 8.7 pg/ml ; p < .0001) .	0.999	0.81
lung cancer	MUC16	the mean concentration of ca 125 was higher in patients with lung cancer (37 + / - 81 u/ml) than in those with nonmalignant disease (4.2 + / - 5.7 u/ml) (p less than 0.01) .	0.999	0.806
prostate cancer	AR	the androgen receptor was expressed in all primary and metastatic prostate cancer tissues and no mutations were identified .	0.999	0.801

Disease Name	Gene Symbol	Text	Before Calibration	After Calibraiton
breast cancer	ERBB2	the results of multiple linear regression analysis , with her2 as the dependent variable , showed that family history of breast cancer was significantly associated with elevated her2 levels in the tumors (p = 0.0038) , after controlling for the effects of age , tumor estrogen receptor , and dna index .	0.999	0.8

Table 4: Contains the bottom ten Disease-associates-Gene confidence scores before and after model calbration. Disease mentions are highlighted in brown and Gene mentions are highlighted in blue.

Disease Name	Gene Symbol	Text	Before Calibration	After Calibraiton
breast cancer	NAT2	[the relationship between passive smoking , breast cancer risk and n-acetyltransferase 2 (nat2)] .	0.012	0.287
schizophrenia	EP300	ventricle size and p300 in schizophrenia .	0.012	0.286
hematologic cancer	CD33	in the 2 (nd) study of cd33 + sr-aml 2 doses of go (4.5 - 9 mg/m (2)) were administered > = 60d post reduced intensity conditioning (ric) allosct (8 wks apart) .	0.01	0.281
Crohn's disease	PTPN2	in this sample , we were able to confirm an association between cd and ptpn2 (genotypic p = 0.019 and allelic p = 0.011) , and phenotypic analysis showed an association of this snp with late age at first diagnosis , inflammatory and penetrating cd behaviour , requirement of bowel resection and being a smoker at diagnosis .	0.008	0.268
breast cancer	ERBB2	long-term efficacy and safety of adjuvant trastuzumab for her2-positive early [breast cancer] .	0.007	0.262
hematologic cancer	CD40LG	we examined the direct effect of lenalidomide on cll-cell proliferation induced by cd154-expressing accessory cells in media containing interleukin-4 and -10 .	0.006	0.259
hematologic cancer	MLANA	methods : the sln sections (n = 214) were assessed by qrt assay for 4 established messenger rna biomarkers : mart-1 , mage-a3 , galnac-t , and pax3 .	0.005	0.252
breast cancer	ERBB2	the keywords erbb2 or her2 or erbb-2 or her-2 and breast cancer and (country) were used to search pubmed , international and local conference abstracts and local-language journals from the year 2000 onwards .	0.003	0.225
hepatitis B	PKD2	conversely , a significant enhancement of activation was observed for afb1 in cases of mild cah and especially for trp-p-2 in hepatitis b virus carriers , irrespective of their histologic diagnosis .	0.002	0.217
hematologic cancer	C7	serum antibody responses to four haemophilus influenzae type b capsular polysaccharide-protein conjugate vaccines (prp-d , hboc , c7p , and prp-t) were studied and compared in 175 infants , 85 adults and 140 2-year-old children .	0.002	0.208

Table 5: Contains the top ten Compound-treats-Disease confidence scores after model calbration. Disease mentions are highlighted in brown and Compound mentions are highlighted in red.

Compound Name	Disease Name	Text	Before Calibration	After Calibration

Compound Name	Disease Name	Text	Before Calibration	After Calibration
Methylprednisolone	asthma	use of tao without methylprednisolone in the treatment of severe asthma .	1.0	0.895
Methyldopa	hypertension	atenolol and methyldopa in the treatment of hypertension .	1.0	0.888
Prednisone	asthma	prednisone and beclomethasone for treatment of asthma .	1.0	0.885
Prazosin	hypertension	experience with prazosin in the treatment of hypertension .	1.0	0.883
Prazosin	hypertension	prazosin in the treatment of hypertension .	1.0	0.878
Prazosin	hypertension	prazosin in the treatment of [hypertension] .	1.0	0.878
Methyldopa	hypertension	oxprenolol plus cyclopenthiazide-kcl versus methyldopa in the treatment of hypertension .	1.0	0.877
Prednisolone	lymphatic system cancer	peptichemio : a new oncolytic drug in combination with vincristine and prednisolone in the treatment of non-hodgkin lymphomas .	1.0	0.871
Methyldopa	hypertension	methyldopate , the ethyl ester hydrochloride salt of alpha-methyldopa (alpha-md) , is used extensively in the treatment of severe hypertension .	1.0	0.851
Haloperidol	Gilles de la Tourette syndrome	a comparison of pimozide and haloperidol in the treatment of gilles de la tourette 's syndrome .	1.0	0.839

Table 6: Contains the bottom ten Compound-treats-Disease confidence scores before and after model calbration. Disease mentions are highlighted in brown and Compound mentions are highlighted in red.

Compound Name	Disease Name	Text	Before Calibration	After Calibration
Dexamethasone	hypertension	dexamethasone and hypertension in preterm infants .	0.011	0.34
Reserpine	hypertension	reserpine in hypertension : present status .	0.01	0.336
Creatine	coronary artery disease	scintiphotographic findings were compared with the size of myocardial infarcts calculated from measurements of the activity of mb isoenzymes of creatine kinase (ck-mb) in serum and in the myocardium at autopsy , as described by sobel 's method .	0.009	0.334
Hydrocortisone	brain cancer	to explore the effects of repeated episodes of hypercortisolemia on hypothalamic-pituitary-adrenal axis regulation , we studied plasma acth and cortisol (cort) responses to 100 micrograms human crh (hcrh) in 10 dexamethasone (1.5 mg) - pretreated elderly endurance athletes who had abstained from physical activity for at least 48 h before testing and 13 sedentary age-matched controls .	0.009	0.333
Hydrocortisone	brain cancer	basal activity of the hypothalamic-pituitary-adrenal axis was estimated by determinations of 24-h urinary free cortisol-excretion , evening basal plasma total and free cortisol concentrations , and the cortisol binding globulin-binding capacity .	0.008	0.328

Compound Name	Disease Name	Text	Before Calibration	After Calibration
Creatine	coronary artery disease	during successful and uncomplicated angioplasty (ptca) , we studied the effect of a short lasting myocardial ischemia on plasma creatine kinase , creatine kinase mb-activity , and creatine kinase mm-isoforms (mm1 , mm2 , mm3) in 23 patients .	0.006	0.318
Benzylpenicillin	epilepsy syndrome	it was shown in experiments on cats under nembutal anesthesia that a lesion of the medial forebrain bundle (mfb) and partly of the preoptic region at the side of local penicillin application on the cerebral cortex (g. suprasylvius medius) results in depression of the epileptiform activity in the penicillin-induced focus , as well as in the secondary " mirror " focus , which appeared in the symmetrical cortex area of the other hemisphere .	0.005	0.315
Indomethacin	hypertension	effects of indomethacin in rabbit renovascular hypertension .	0.004	0.308
Cyclic Adenosine Monophosphate	ovarian cancer	the hormonal regulation of steroidogenesis and adenosine 3 ' :5 ' - cyclic monophosphate in embryonic-chick ovary .	0.002	0.292
Dobutamine	coronary artery disease	two-dimensional echocardiography can detect regional wall motion abnormalities resulting from myocardial ischemia produced by dobutamine infusion .	0.002	0.287

Table 7: Contains the top ten Compound-treats-Disease confidence scores before and after model calbration. Gene mentions are highlighted in blue and Compound mentions are highlighted in red.

Compound Name	Gene Symbol	Text	Before Calibration	After Calibration
Hydrocortisone	SHBG	serum concentrations of testicular and adrenal androgens and androgen precursors , cortisol , unconjugated (e1) and total estrone (te1 ; greater than or equal to 85 % e1 sulfate) , pituitary hormones , sex hormone binding globulin (shbg) and albumin were measured in 14 male patients with non-diabetic end stage renal disease and in 28 age-matched healthy controls .	0.997	0.745
Minoxidil	EGFR	direct measurement of the ability of minoxidil to compete for binding to the egf receptor indicated that minoxidil probably does not bind to the egf receptor .	0.99	0.706
Hydrocortisone	SHBG	gonadotropin , testosterone , sex hormone binding globulin (shbg) , dehydroepiandrosterone sulphate , androstenedione , estradiol , prolactin , cortisol , thyrotropin , and free thyroxine levels were determined .	0.988	0.7
Cholecalciferol	DBP	cholecalciferol (vitamin d3) and its 25-hydroxy metabolite are transported in plasma bound to a specific protein , the binding protein for cholecalciferol and its metabolites (dbp) .	0.983	0.685
Indomethacin	AGT	indomethacin , a potent inhibitor of prostaglandin synthesis , is known to increase the maternal blood pressure response to angiotensin ii infusion .	0.982	0.68

Compound Name	Gene Symbol	Text	Before Calibration	After Calibration
Tretinoin	RXRA	the vitamin a derivative retinoic acid exerts its effects on transcription through two distinct classes of nuclear receptors , the retinoic acid receptor (rar) and the retinoid x receptor (rxr) .	0.975	0.668
Dopamine	NTS	neurotensin binding was not modified by the addition of dopamine .	0.97	0.659
D-Tyrosine	PLCG1	epidermal growth factor (egf) or platelet-derived growth factor binding to their receptor on fibroblasts induces tyrosine phosphorylation of plc gamma 1 and stable association of plc gamma 1 with the receptor protein tyrosine kinase .	0.969	0.659
D-Tyrosine	PLCG1	tyrosine phosphorylation of plc-ii was stimulated by low physiological concentrations of egf (1 nm) , was quantitative , and was already maximal after a 30 sec incubation with 50 nm egf at 37 degrees c. interestingly , antibodies specific for plc-ii were able to coimmunoprecipitate the egf receptor and antibodies against egf receptor also coimmunoprecipitated plc-ii .	0.964	0.651
Ketamine	C5	additionally , reduction of glycine binding by the c-5 antagonists was reversed by both nmda receptor agonists and c-7 competitive nmda antagonists , providing evidence that the site of action of these c-5 antagonists is the nmda recognition site , resulting in indirect modulation of the glycine site .	0.957	0.643

Table 8: Contains the bottom ten Compound-binds-Gene confidence scores before and after model calbration. Gene mentions are highlighted in blue and Compound mentions are highlighted in red.

Compound Name	Gene Symbol	Text	Before Calibration	After Calibration
Iron	NDUFB3	since gastric acid plays an important role in the absorption process of iron and vitamin b12 , we determined levels of iron , ferritin , vitamin b12 , and folic acid in 75 serum samples obtained during continuous omeprazole therapy (6-48 months after start of therapy) from 34 patients with peptic diseases (primarily reflux esophagitis) .	0.006	0.276
D-Tyrosine	PLAU	either the 55 kda u-pa form and the lower mw form (33 kda) derived from the 55 kda u-pa are tyr-phosphorylated also the u-pa secreted in the culture media of human fibrosarcoma cells (ht-1080) is phosphorylated in tyrosine as well as u-pa present in tissue extracts of tumors induced in nude mice by ht-1080 cells .	0.006	0.276
D-Leucine	POMC	cross-reactivities of leucine-enkephalin and beta-endorphin with the eia were less than 0.1 % , while that with gly-gly-phe-met and oxidized gly-gly-phe-met were 2.5 % and 10.2 % , respectively .	0.006	0.273
Eprazinone	GAST	in patients with renal failure there exists the inhibition of the gastrin acid secretion which is the cause of the weakening of the mechanism of the feedback connection between hcl and gastrin , while because of a permanent stimulation of g-cells , the hyperplasia of these cells develops , as well as the increased secretory activity , and hypergastrinemia .	0.005	0.271

Compound Name	Gene Symbol	Text	Before Calibration	After Calibration
Hydrocortisone	GH1	luteinizing hormone responses to luteinizing hormone releasing hormone , and growth hormone and cortisol responses to insulin induced hypoglycaemia in functional secondary amenorrhoea .	0.005	0.271
Hydrocortisone	GH1	group iv patients had normal basal levels of lh and normal lh , gh and cortisol responses .	0.005	0.269
Bupivacaine	AVP	plasma renin activity and vasopressin concentration , arterial pressure , and serum osmolality were measured in 17 patients before and after random epidural injection of either 6.7 ml of 0.75 % bupivacaine (n = 7) or the same volume of saline (n = 10) .	0.004	0.26
Epinephrine	INS	thermogenic effect of thyroid hormones : interactions with epinephrine and insulin .	0.004	0.259
Hydrocortisone	GH1	cortisol and growth hormone (gh) secretion (spontaneous variations at night and the release induced by insulin hypoglycaemia) were investigated in 69 children and adolescents .	0.002	0.241
Estriol	LGALS1	[diagnostic value of serial determination of estriol and hpl in plasma and of total estrogens in 24-h-urine compared to single values for diagnosis of fetal danger] .	0.0	0.181

Table 9: Contains the top ten Gene-interacts-Gene confidence scores before and after model calbration. Both gene mentions highlighted in blue.

Gene1 Symbol	Gene2 Symbol	Text	Before Calibration	After Calibration
INS	HSPA4	conclusions : intact insulin only weakly interacts with the hsp70 chaperone dnak whereas monomeric proinsulin and peptides from 3 distinct proinsulin regions show substantial chaperone binding .	0.834	0.574
NMT1	S100B	values for k (cat) indicated that , once gag or nef binds to the enzyme , myristoylation by nmt1 and nmt2 proceeds at comparable rates .	0.826	0.571
VEGFA	HIF1A	mechanistically , we demonstrated that resveratrol inhibited hif-1alpha and vegf expression through multiple mechanisms .	0.82	0.569
ITGAV	PECAM1	antigens expressed on emp and ec were assayed flow cytometrically and included constitutive markers (cd31 , cd51/61 , cd105) , inducible markers (cd54 , cd62e and cd106) , and annexin v binding .	0.81	0.566
F10	PF4	these compounds inhibit both factor xa and thrombin , in the presence of antithrombin , while they are devoid of undesirable non-specific interactions , particularly with platelet factor 4 (pf4) .	0.766	0.554
NFKB2	RELB	the results indicate that dystrophic muscle is characterized by increases in the whole cell expression of ikappab-alpha , p65 , p50 , relb , p100 , p52 , ikk , and traf-3 .	0.76	0.553
SSSCA1	CDKN1B	conclusion : hl-60 / ht cells have lower p27 (kip1) expression compared with hl-60 cells .	0.757	0.552

Gene1 Symbol	Gene2 Symbol	Text	Before Calibration	After Calibration
PTH2R	PTH2	thus , the juxtamembrane receptor domain specifies the signaling and binding selectivity of tip39 for the pth2 receptor over the pth1 receptor .	0.749	0.55
MMP9	MMP2	all these factors markedly influenced the secretion and/or activation of mmp-2 and mmp-9 .	0.738	0.547
CCND1	ABL1	synergy with v-abl depended on a motif in cyclin d1 that mediates its binding to the retinoblastoma protein , suggesting that abl oncogenes in part mediate their mitogenic effects via a retinoblastoma protein-dependent pathway .	0.736	0.547

Table 10: Contains the bottom ten Gene-interacts-Gene confidence scores before and after model calbration. Both gene mentions highlighted in blue.

| Gene1 Symbol	Gene2 Symbol	Text	Before Calibration	After Calibration
IFNG	IL6	in the control group , the positive rate for il-4 , il-6 , il-10 were 0/10 , 2/10 and 1/10 , respectively , and those for il-2 and ifn-gamma were both 1/10 .	0.012	0.306
ACHE	BCHE	anticholinesterase activity was determined against acetylcholinesterase (ache) and butyrylcholinesterase (bche) , the enzymes vital for alzheimer 's disease , at 50 , 100 and 200 g ml (-1) .	0.011	0.306
CCL2	AGT	we found no significant increase in mcp-1 concentrations by ang ii alone ; but it enhanced the tnf-alpha-induced mcp-1 mrna expression in a dose-dependent manner .	0.011	0.306
CXCL8	IL1B	furthermore , somatostatin completely abrogated the increased secretion of il-8 and il-1beta after invasion by salmonella .	0.011	0.303
SULT1A2	SULT1A3	to date , the laboratory has cloned seven unique human sulfotransferases ; five aryl sulfotransferases (hast1 , hast2 , hast3 , hast4 and hast4v) , an estrogen sulfotransferase and a dehydroepiandrosterone sulfotransferase .	0.009	0.295
IFNG	IL10	results : we found weak mrna expression of interleukin-4 (il-4) and il-5 , and strong expression of il-6 , il-10 and ifn-gamma before therapy .	0.008	0.292
IL2	IFNG	prostaglandin e2 at priming of naive cd4 + t cells inhibits acquisition of ability to produce ifn-gamma and il-2 , but not il-4 and il-5 .	0.007	0.289
IL2	IFNG	the detailed distribution of lymphokine-producing cells showed that il-2 and ifn-gamma-producing cells were located mainly in the follicular areas .	0.007	0.287
IL2	IFNG	pbl of ms patients produced more pro-inflammatory cytokines , il-2 , ifn-gamma and tnf/lymphotoxin , and less anti-inflammatory cytokine , tgf-beta , during wk 2 to 4 in culture than pbl of normal controls .	0.006	0.283
NFKB1	TNF	nf-kappab-dependent reporter gene transcription activated by tnf was also suppressed by calagualine .	0.005	0.276

Baseline Comparison
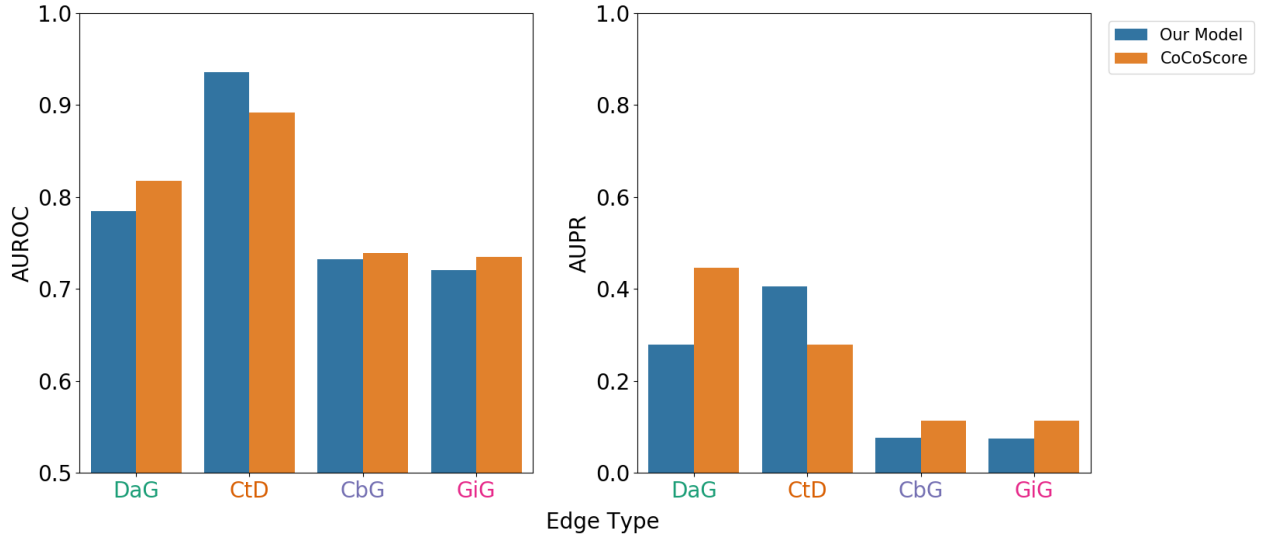
Figure 10: Comparion between our model and CoCoScore model [13]. We report both model's performance in terms of AUROC and AUPR. Our model achieves comparable performance against CoCoScore in terms of AUROC. As for AUPR, CoCoScore consistently outperforms our model except for CtD.

Once our discriminator model is calibrated, we grouped sentences based on mention pair (edges). We assigned each edge the maximum score over all grouped sentences and compared our model's ability to predict pairs in our test set to a previously published baseline model [13]. Performance is reported in terms of AUROC and AUPR (Figure 10). Across edge types our model shows comparable performance against the baseline in terms of AUROC. Regarding AUPR, our model shows hindered performance against the baseline. The exception for both cases is CtD where our model performs better than the baseline.

Reconstructing Hetionet
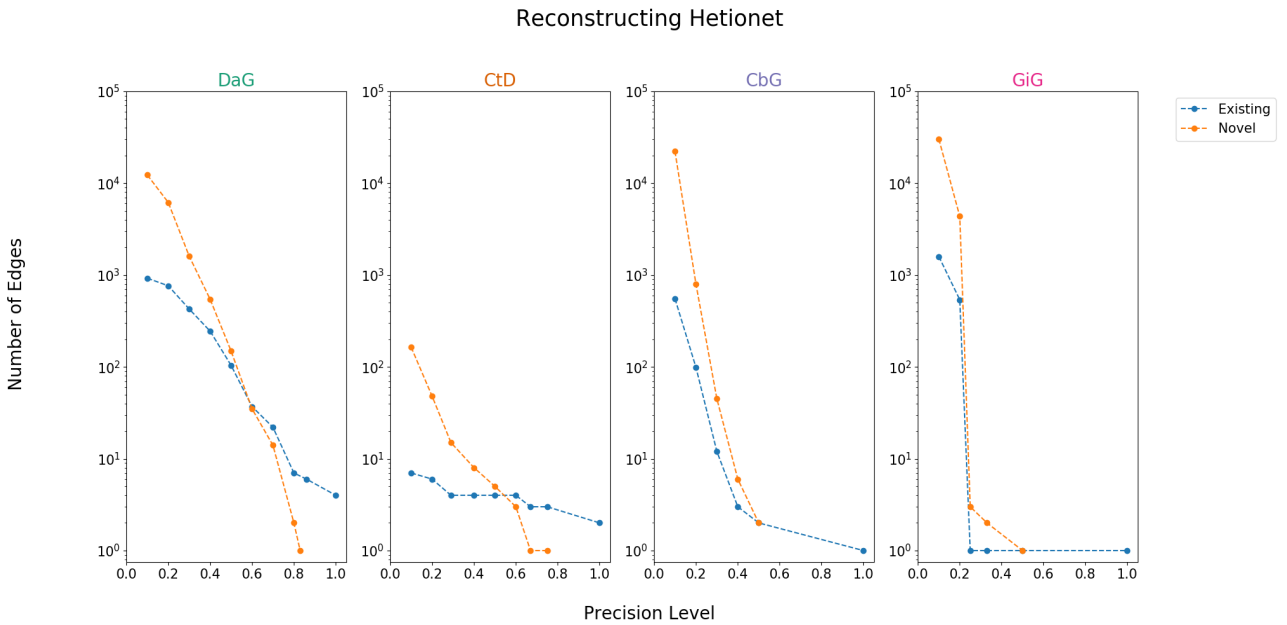
Figure 11: A scatter plot showing the number of edges (log scale) we can add or recall at specified precision levels. The blue depicts edges existing in hetionet and the orange depicts how many novel edges can be added.

We evaluated how many edges we can recall/add to Hetionet v1 (Supplemental Figure 11 and Table 11). In our evaluation we used edges assigned to our test set. Overall, we can recall a small amount of edges at high precision thresholds. A key example is CbG and GiG where we recalled only one exisiting

edge at 100% precision. Despite the low recall, we are still able to add novel edges to DaG and CtD while retaining modest precision.

Table 11: Contains the top ten predictions for each edge type. Highlighted words represent entities mentioned within the given sentence.

Edge Type	Source Node	Target Node	Gen Model Prediction	Disc Model Prediction	Number of Sentences	Text
DaG	lung cancer	VEGFA	1.000	0.912	3293	conclusion : the plasma vegf level is increased in nsclc patients with approximate1y one fourth to have cancer cells in the peripheral blood.
DaG	hematologic cancer	TP53	1.000	0.905	8660	mutations of the p53 gene were found in four cases of cml in blastic crisis (bc).
DaG	obesity	MC4R	1.000	0.901	1493	several mutations in the melanocortin 4 receptor gene are associated with obesity in chinese children and adolescents.
DaG	Alzheimer's disease	VLDLR	1.000	0.886	86	the 5-repeat allele in the very-low-density lipoprotein receptor gene polymorphism is not increased in sporadic alzheimer 's disease in japanese.
DaG	lung cancer	XRCC1	1.000	0.885	662	results : xrcc1 gene polymorphism is associated with increased risk of lung cancer when the arg/arg genotype was used as the reference group.
DaG	prostate cancer	ESR1	1.000	0.883	500	conclusion : these results suggest that variants of the ggga polymorphism from the estrogen receptor alpha gene may be associated with an increased risk of developing prostate cancer.
DaG	breast cancer	REG1A	1.000	0.878	37	conclusion : high levels of reg1a expression within tumors are an independent predictor of poor prognosis in patients with breast cancer.
DaG	breast cancer	INSR	1.000	0.877	200	we have previously reported that insulin receptor expression is increased in human breast cancer specimens (v. papa et al. , j. clin.

Edge Type	Source Node	Target Node	Gen Model Prediction	Disc Model Prediction	Number of Sentences	Text
DaG	rheumatoid arthritis	AR	1.000	0.877	53	conclusion : our results suggest no correlation between cag repeat polymorphism in the ar gene and response to treatment with lef in women with ra.
DaG	coronary artery disease	CTLA4	1.000	0.875	12	conclusion : the g/g genotype polymorphism of the ctla-4 gene is associated with increased risk of ami.
CtD	Zonisamide	epilepsy syndrome	1.000	0.943	1011	adjunctive zonisamide therapy in the long-term treatment of children with partial epilepsy : results of an open-label extension study of a phase iii , randomized , double-blind , placebo-controlled trial.
CtD	Metformin	polycystic ovary syndrome	1.000	0.942	3217	in the present study , 23 pcos subjects [mean (+ / - se) body mass index 30.0 + / -1.1 kg/m2] were randomly assigned to double-blind treatment with metformin (500 mg tid) or placebo for 6 months , while maintaining their usual eating habits.
CtD	Piroxicam	rheumatoid arthritis	1.000	0.928	184	methods : a double-blind , randomized , crossover trial in 49 patients with active ra compared 6 weeks of treatment with tenidap (120 mg/day) versus 6 weeks of treatment with piroxicam (20 mg/day).
CtD	Irinotecan	stomach cancer	1.000	0.918	968	randomized phase ii trial of first-line treatment with tailored irinotecan and s-1 therapy versus s-1 monotherapy for advanced or recurrent gastric carcinoma (jfmc31-0301).
CtD	Treprostinil	hypertension	1.000	0.913	536	oral treprostinil for the treatment of pulmonary arterial hypertension in patients receiving background endothelin receptor antagonist and phosphodiesterase type 5 inhibitor therapy (the freedom-c2 study) : a randomized controlled trial.

Edge Type	Source Node	Target Node	Gen Model Prediction	Disc Model Prediction	Number of Sentences	Text
CtD	Colchicine	gout	1.000	0.911	78	this is the first in vivo data to provide a biological rationale that supports the implementation of low dose , non-toxic , colchicine therapy for the treatment of gouty arthritis.
CtD	Propranolol	stomach cancer	1.000	0.898	45	74 cirrhotic patients with a history of variceal or gastric bleeding were randomly assigned to treatment with propranolol (40 to 360 mg/day) or placebo.
CtD	Reboxetine	endogenous depression	1.000	0.894	439	data were obtained from four short-term (4-8-week) , randomized , placebo-controlled trials of reboxetine for the treatment of mdd.
CtD	Diclofenac	ankylosing spondylitis	1.000	0.892	61	comparison of two different dosages of celecoxib with diclofenac for the treatment of active ankylosing spondylitis : results of a 12-week randomised , double-blind , controlled study.
CtD	Tapentadol	osteoarthritis	1.000	0.880	29	driving ability in patients with severe chronic low back or osteoarthritis knee pain on stable treatment with tapentadol prolonged release : a multicenter , open-label , phase 3b trial.
CbG	Dexamethasone	NR3C1	1.000	0.850	1119	submicromolar free calcium modulates dexamethasone binding to the glucocorticoid receptor.
CbG	Vitamin A	RBP4	1.000	0.807	5512	the authors give serum retinol binding protein (rbp) normal values , established by immunonephelometry , for two healthy populations in their hospital laboratory.
CbG	D-Proline	IGFBP4	1.000	0.790	1	the insulin-like growth factor-i-stimulated l-proline uptake was inhibited by one of its binding protein , insulin-like growth factor binding protein-4 , in a concentration-dependent manner.

Edge Type	Source Node	Target Node	Gen Model Prediction	Disc Model Prediction	Number of Sentences	Text
CbG	Sucrose	AR	0.996	0.789	37	the amount (maximal binding capacity of 24 to 30 fmol/mg protein) and hormone binding affinity (half-maximal saturation of 0.2 nm) of the androgen receptor in cultured skin fibroblasts was normal , but the receptor was qualitatively abnormal as evidenced by instability on sucrose density gradient centrifugation.
CbG	D-Lysine	PLG	1.000	0.787	403	in both elisa and rocket immunoelectrophoresis systems , complex formation was inhibited by 10 mm epsilon-amino-n-caproic acid , implying that there is a role for the lysine binding sites of plg in mediating the interaction.
CbG	Adenosine	INSR	1.000	0.785	129	these findings demonstrate basal state binding of atp to the ckd leading to cis-autophosphorylation and novel basal state regulatory interactions among the subdomains of the insulin receptor kinase.
CbG	Adenosine	PLK1	1.000	0.783	104	most kinase inhibitors interact with the atp binding site on plk1 , which is highly conserved.
CbG	Calcium Chloride	ITPR3	0.995	0.777	1954	control of ca2 + influx in human neutrophils by inositol 1,4,5-trisphosphate (ip3) binding : differential effects of micro-injected ip3 receptor antagonists.
CbG	D-Arginine	C5AR1	1.000	0.775	808	thus , selected out of a multiplicity of possibilities by the natural binding partner , arg37 as well as arg40 appear to be anchor residues in binding to the c5a receptor.
CbG	Ticagrelor	P2RY12	1.000	0.773	322	purpose : ticagrelor is a reversibly binding p2y12 receptor antagonist used clinically for the prevention of atherothrombotic events in patients with acute coronary syndromes (acs).

Edge Type	Source Node	Target Node	Gen Model Prediction	Disc Model Prediction	Number of Sentences	Text
GiG	ABL1	ABL1	0.999	0.600	9572	the acquired resistance in patients who failed to respond to imatinib seemed to be induced by several point mutations in the bcr-abl gene , which were likely to affect the binding of imatinib with bcr-abl.
GiG	TP63	TP53	1.000	0.595	2557	tp63 , a member of the p53 gene family gene , encodes the np63 protein and is one of the most frequently amplified genes in squamous cell carcinomas (scc) of the head and neck (hnscc) and lungs (lusc).
GiG	FERMT1	FERMT1	0.004	0.590	194	ks is caused by mutations in the fermt1 gene encoding kindlin-1.
GiG	GRN	GRN	1.000	0.590	3842	background : mutations in the progranulin gene (pgrn) have recently been identified as a cause of frontotemporal lobar degeneration with ubiquitin-positive inclusions (ftld-u) in some families.
GiG	FASN	EP300	0.999	0.589	6	here , we demonstrated that p300 binds to and increases histone h3 lysine 27 acetylation (h3k27ac) in the fasn gene promoter.
GiG	SETBP1	SETBP1	1.000	0.588	354	the critical deleted region contains setbp1 gene (set binding protein 1).
GiG	BCL2	BAK1	0.118	0.587	1220	different expression patterns of bcl-2 family genes in breast cancer by estrogen receptor status with special reference to pro-apoptotic bak gene.
GiG	SP1	INSR	0.948	0.587	23	thus , the efficient expression of the human insulin receptor gene possibly requires the binding of transcriptional factor sp1 to four g-c boxes located -593 to -618 base pairs upstream of the atg translation initiation codon.

Edge Type	Source Node	Target Node	Gen Model Prediction	Disc Model Prediction	Number of Sentences	Text
GiG	ABCD1	ABCD1	1.000	0.586	410	x-linked adrenoleukodystrophy (x-ald) is caused by mutations in the abcd1 gene encoding the peroxisomal abc transporter adrenoleukodystrophy protein (aldp).
GiG	CYP1A1	AHR	0.996	0.586	1940	the liganded ah receptor activates transcription by binding to a specific dna-recognition motif within a dioxin-responsive enhancer upstream of the cyp1a1 gene.

1. Labeled sentences are available [here](#).↩